UNITED NATIONS UNIVERSITY
GEOTHERMAL TRAINING PROGRAMME
Orkustofnun, Grensásvegur 9,
IS-108 Reykjavík, Iceland

Reports 2007
Number 14

INTERPRETATION OF EXPLORATION GEOCHEMICAL DATA FOR GEOTHERMAL FLUIDS FROM THE GEOTHERMAL FIELD OF THE RUNGWE VOLCANIC AREA, SW-TANZANIA

Taramaeli T. Mnjokava
Geological Survey of Tanzania
Kikuyu Avenue / Boma Road
P.O. Box 903, Dodoma
TANZANIA
mnjott@yahoo.co.uk

ABSTRACT

The Rungwe volcanic field in the Mbeya region, SW-Tanzania is known for its hot springs, the common manifestations of a geothermal energy source. This study is a part of the search for a potential high-enthalpy reservoir in this region. Chemical analysis for solutes in water samples from the Rungwe volcanic hot springs and caldera water from Lake Ngozi were used for interpretation in this report.

The chemical characteristics of the hot springs were evaluated using Cl-SO_4-HCO_3, Li-Cl-B and Na-K-Mg ternary diagrams. All waters have low B/Cl ratios, suggesting that they are derived from an old hydrothermal system. Three groups of waters can be distinguished on the basis of predictions of subsurface temperatures with geothermometers. The first group consists of cold springs (Shiwaga, Mulagara and Isebe) which are characterised as immature waters. For these, the use of geothermometers for calculating subsurface temperature is unrealistic. The second group of thermal springs (Kilambo, Mampulo B, Kandete and Kasimulo) is characterised by peripheral partially equilibrated waters with lower predicted Na-K subsurface temperatures, but with higher temperatures (calculated with silica geothermometers) than the third group (Songwe hot springs: Ilatile 1, River spring, Ilatile 4 and Main spring B). The quartz, chalcedony and Na-K temperatures were calculated by the WATCH computer program and the Na-K-Ca temperature by the SOLVEQ computer program.

Log (Q/K) diagrams show the range and cluster of equilibrium temperatures which, in most cases, are close to the chalcedony temperature. With the exception of two springs from the second group (Kandete and Kasimulo), the chalcedony temperature estimates lie within the subsurface temperature range estimated from the log (Q/K) diagrams. The silica-enthalpy model predicts maximum subsurface temperatures for the most prominent springs of the second group (Kandete and Kasimulo).

1. INTRODUCTION

The two year project (2006-2008) "Geothermal as an Alternative Source of Energy for Tanzania" was initiated by the Ministry of Energy and Minerals (MEM), the Geological Survey of Tanzania (GST)

and the Federal Institute for Geosciences and Natural Resources (BGR), Germany in June 2006. Capacity building, the main project component, comprises training Tanzanian experts in acquiring, analysing and interpreting the geothermal exploration data. It was through this project that the author was given the opportunity to attend a six month course at the United Nations University Geothermal Training Programme (UNU-GTP) in Reykjavík, Iceland from April to October 2007, specializing in the Chemistry of Thermal Fluids.

Several reconnaissance surveys and studies of geothermal energy in Tanzania have shown a geothermal energy source potential (McNitt, 1982; Hochstein at al., 2000). The studies were based on the natural heat discharge of hot springs. However, the geothermal resource has not been used up to now and has only been explored to a small extent. The Rungwe volcanic field has been considered for further geothermal investigations. The challenge is to locate the geothermal reservoirs by integrating modern exploration techniques such as geophysical, geochemical and geological methods.

Fluid geochemistry is an important tool during all stages of geothermal development and production. The existence of geothermal reservoirs in a particular area is manifested by the presence of thermal springs and /or fumaroles. Geothermal exploration has, however, revealed that hidden reservoirs also exist. Thus, it is important to locate geothermal areas favourable to development and to find sites within them for drilling. The principal objective of geochemical surveys during geothermal exploration is to predict subsurface temperatures, to obtain information on the origin of the geothermal fluid and to understand subsurface flow directions (Arnórsson, 2000a). Geochemical studies of geothermal fluids essentially involve three steps, namely: sampling, analysis and data interpretation.

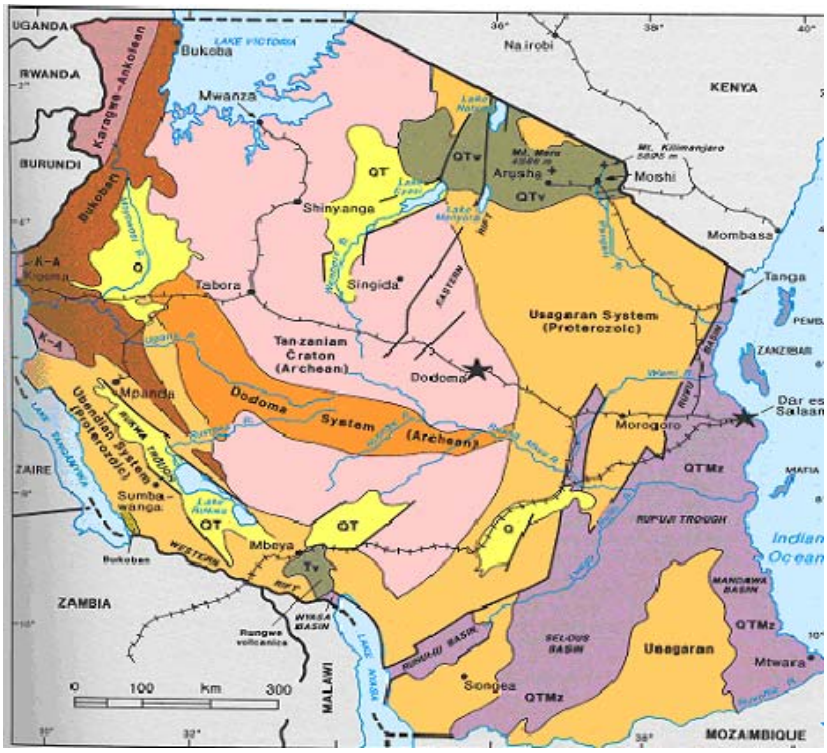

FIGURE 1: A simplified geological map of Tanzania (htt://Tanzania.sgu.se/IMAGES/map.htm)

Figure 1 shows a simplified geological map of Tanzania. The study area is in the Rungwe volcanic field located close to Mbeya, SW-Tanzania (Figure 2). The geothermal sites in this region are hot springs located in three basins around the volcanic field, in Rukwa, Malawi and Usangu Basin (Figure 3). The sites include: Songwe hot springs, Mampulo, Kasimulo, Kilambo, Ilatile 1, Ilatile 4, Shiwaga, Mulagara, Kandete, Isebe, Swaya and Lake Ngozi. The fluid samples, collected during field work conducted at these sites, were analysed in the BGR laboratory and were used for this study.

This report, as a part of the course in Chemistry of Thermal Fluids at UNU-GTP, has the objective of interpreting the geochemical exploration data from the geothermal field of the Rungwe volcanic area, SW-Tanzania, by applying geochemical methodology outlined in Section 3 of this report. Most computations were performed with the SOLVEQ (Reed and Spycher, 1984; Spycher and Reed, 1989) and WATCH (Arnórsson et al., 1982; Bjarnason, 1994) programs. The evaluation of the hot springs is given in Section 4.

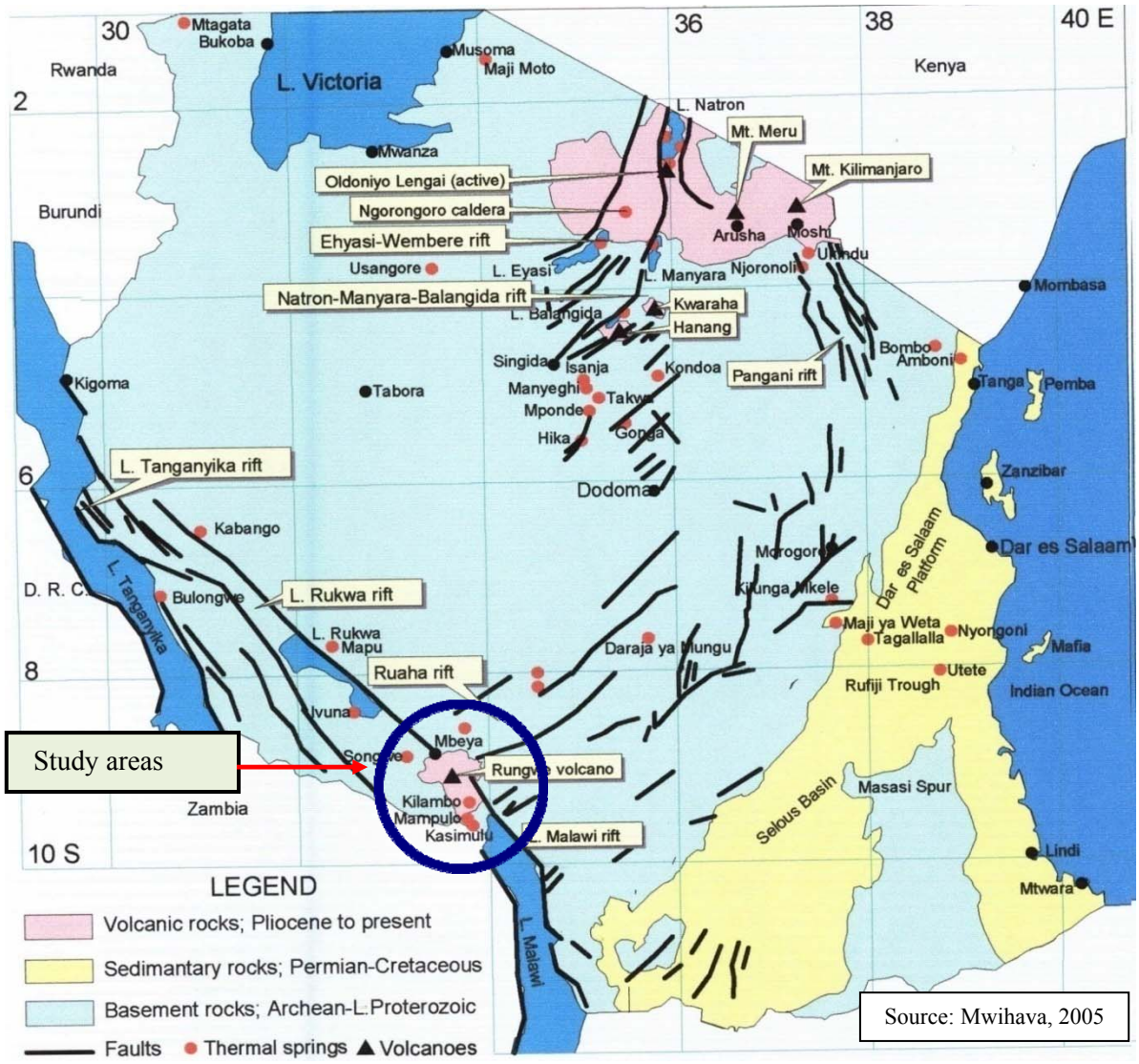

FIGURE 2: Geothermal sites, study area and the rifting system in Tanzania

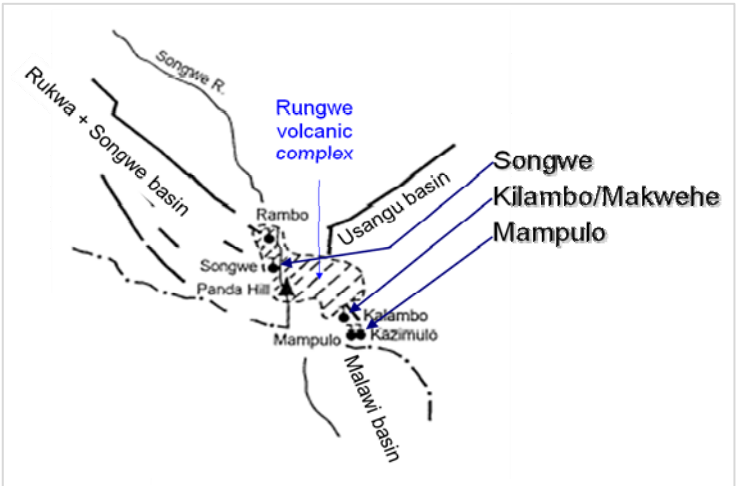

FIGURE 3: Triple junction at the Rungwe volcanic complex and a few thermal areas sampled (Pisarskii et al., 1998)

2. STUDY AREAS

The study areas are located in the Mbeya region, in the southwest part of Tanzania. Geochemical sampling extends from Songwe (northwest of Mbeya town) and covers the volcanic area of Ngozi, Kiejo and Tukuyu up to the northern part of Lake Nyasa (Figure 2). Accessibility for field measurements is very difficult towards the Ngozi and Rungwe volcanoes due to rugged and steep terrain, with the exception of paved roads.

2.1 Geological setting

The geology of Tanzania (Figure 1) is dominated by a large mineralized Precambrian craton with formations more than 2 billion years old, rimmed by Proterozoic crystalline rocks – the Ubendian System to the west and the Usagaran System to the east. Cenozoic sediments and volcanic rocks fill the inland basins and occur along the coastal plain. These sediments and volcanics are related to the active Cenozoic East African System which is divided into a western and an eastern branch (Figure 2). The two branches form a triple junction at the Rungwe volcanic complex (Delvaux and Hanon, 1993) in the Mbeya area (Figure 3). The triple junction of the NW-SE trending South Rukwa and North Malawi Rift basins intersected by the younger NE-SW trending Usangu basin is covered by Rungwe volcanic rocks. There is also a number of Cretaceous carbonatite intrusives in the Mbeya region, including the Panda Hill Carbonatite which is located between Ngozi volcano and Songwe hot springs. The conditions for high-enthalpy resources are principally favourable in the Mbeya region due to the presence of active faults allowing fluid flow, young volcanic heat sources (which are sparse in other areas of the western branch of the East African Rift System) and the occurrence of surface manifestations (e.g. hot springs (Figure 2) indicating subsurface geothermal activity.

2.2 Hot springs and previous geothermal studies

Preliminary investigations of geothermal springs in the study areas have been described by Harkin (1960); James (1967); Walker (1969); SWECO (1978); McNitt (1982); Makundi and Kifua (1985); Pisarskii, et al. (1998); Hochstein et al. (2000); Mnzava et al. (2004); Mwihava et al. (2004); Hochstein (2005); Branchu et al. (2005); and DECON et al. (2005). Moderate hydrothermal activity occurs over and adjacent to the Rungwe volcanic field which mainly consists of alkali-basaltic and trachytic/phenolitic rocks of Miocene to Quaternary age. To the northeast of the Rungwe volcanic field lies a young sedimentary basin – the Usangu basin (Figure 3), created by rifting (Ebinger et al., 1989). A few minor hot springs occur at its margins (Walker, 1969).

In the northern extension of the Malawi Rift, three reservoirs of intermediate to high temperature are indicated by the occurrence of hot springs at the foot of long, concealed outflows discharging water of neutral pH and bicarbonate water that deposits travertine. The hot and cold water springs are characterized by gas emissions and temperatures ranging from 50 to 80^{o}C. Na and HCO_3 contents of the water are higher than 34 mmol/l and 1400 mmol/l, respectively, with a constant Na/K ratio suggesting a homogenous fluid at depth. The relatively high heat-flow values and chemical composition of the hot spring fluids suggest the presence of a magmatic body at depth (Branchu et al., 2005).

The largest prospect is at Songwe River which transmits approximately 10 MW of heat. The chemical composition of the thermal water, the CO_2 discharge of the greater flow springs, and the travertine, all indicate that the Songwe hot springs mark the terminus of a concealed outflow of hot water, channelled by a confined aquifer (Hochstein et al., 2000). In the Songwe area, four thermal water springs namely Rambo spring, River Spring, Gas Spring and Main Spring, are located on a line trending in a NNW-SSE direction. There is probably a fault buried by travertine (James, 1967). Temperatures of about 100ºC and 122ºC have been indicated by the chalcedony and K/Mg

geothermometers, respectively. The high T (Na/K) value of ~ 255ºC indicates that the thermal water might be derived from a reservoir located far away from the springs (Hochstein et al., 2000). James (1967) argues that the source of the hot springs is related to volcanic activity.

3. METHODOLOGY

3.1 Geothermal fluid sampling

Correct sampling techniques and sample treatment are needed for reliable analysis of components, of both water and steam samples, as all subsequent steps depend upon it. Some on-site measurements during sampling are necessary, and upon storage, the chemical composition of a sample may change, at least that of some components; later analysis – no matter how well done - will not give correct information on the chemical and isotopic compositions of geothermal fluid at the sampling site, if sampling and sample treatment are inadequate. It is important to keep a record of sampling sites, samples collected and a description of sample locations on a field record card or in a field notebook.

A geothermal fluid may consist of: water collected from natural springs or hot-water wells; steam samples from fumaroles or high temperature wells; gas samples from hot pools or bubbling hot and cold springs; and steam and water from wet-steam wells. When collecting samples from springs it is necessary that the water be free-flowing at the sampling spot. If it is not, a sampling pump is needed. Samples collected from hot wells are cooled to ambient temperatures before collection by connecting the tubing to a stainless steel cooling coil placed in a coolant such as cold water. Likewise the steam is passed through a coil which is immersed in cold water to condense the steam and collect the distillate as condensed liquid when collecting samples from high-temperature wells. Dry steam is collected from high-temperature wells. The pressure and temperature at the wellhead are recorded during sampling.

The following sample treatment and rules apply:

(i) Containers are rinsed well before collecting the samples;
(ii) Bottles are filled to the top to get rid of air bubbles;
(iii) Samples for silica analysis should be raw and diluted-Rd;
(iv) Samples for analysis of CO_2, H_2S , pH (if not in the field) and conductivity are kept in amber glass, raw and unfiltered-Ru;
(v) Three other kinds of samples treatment are: filtered and unacidified-Fu for anion determinations, filtered and acidified-Fa for cation determinations, and Fp filtered and precipitated {with $Zn(CH_3COO)_2$} for analysis of SO_4 ;
(vi) Samples for analysis of isotopes (δ^2H, $\delta^{18}O$) are kept in amber bottles, filtered and unacidified. Filtration is carried out using a 0.45 μm filter membrane.

Sometimes a specific sample treatment is needed for a specific analysis.

3.2 Classification of thermal waters

Chemical and isotopic data based on analytical concentrations are sometimes used directly for the interpretation of geothermal fluid properties. However, it is more common for the analytical data to require some treatment before they can be interpreted for specific purposes. Often primary data on conservative components (tracers) can be used directly; they provide information on their own source as well as on the source of the fluid. On the other hand, most interpretation of reactive components, such as the evaluation of mineral saturation and scaling tendencies, requires the computation of species activities. The reactive constituents have also been termed geoindicators; they are useful in

obtaining information on the physical state of geothermal reservoirs such as temperature and steam-to-water ratios (Arnórsson, 2000a).

Examples of non-reactive constituents are the noble gases He and Ar, and the comparatively 'conservative' constituents Cl, B, Li, Rb, Br, Cs, and N_2. Deuterium (^2H) and ^{18}O are the most widely used isotopes in geothermal work. Others are ^3H, which serves as a tool to determine the mean residence time of water, and ^{14}C for older waters. The $\delta^{18}O$ values of geothermal waters are most often higher (less negative) than those of local meteoric water, a trend in $\delta^{18}O - \delta^2H$ diagrams which has been termed "oxygen isotope shift". This has been interpreted as a result of isotopic exchange at high temperature between the water and rock minerals which are richer in $\delta^{18}O$. The values of δ^2H are sometimes constant. Waters with temperature below 100°C generally show very little oxygen isotope shift, if any. When this is the case, ^{18}O can be used as a tracer, like deuterium, for mixing and vapour separation processes. Waters that have attained higher temperatures have generally reacted sufficiently with the rock to produce a significant oxygen isotope shift. Because of the $\delta^{18}O$ shift in some systems, $\delta^{18}O$ distinguishes hot and cold waters more clearly than δ^2H. Unlike $\delta^{18}O$, δ^2H is hardly affected by exchange processes.

Examples of reactive species are Na, K, Mg, Ca and SiO_2 that take part in temperature-dependent interactions with the Al-silicate rock structures generally housing geothermal systems or, for example, H_2, H_2S, CH_4 and CO_2, that are involved in temperature- and pressure-dependent redox reactions with one another or with redox systems (in FeII/FeIII) of the rock phase (Giggenbach, 1991). The boundaries between the two groups are not rigid, as one component can be inert under one set of conditions, for example Cs at temperature > 250°C, but is incorporated into secondary zeolites at lower temperatures. Each of the constituents of geothermal fluids behaves in its own peculiar way and, therefore, if used to the best advantage, will provide unique information.

3.2.1 Origin of geothermal water

Geothermal fluids originate mainly in meteoric water and sea water (Craig, 1963). To determine the recharge to geothermal systems is an important aspect of geothermal investigations. This is done by measuring the hydrogen and oxygen isotope composition of steam and water of geothermal fields; the isotopic ratio is the number of atoms of a given isotope divided by the number of atoms of the most abundant isotope of that element. It is not easy to measure absolute isotopic ratios accurately, but differences in isotopic ratios between a particular sample and a standard can be measured accurately. For this reason isotopic concentrations are conveniently expressed in the delta notation (δ) as per thousand, or

$$\delta = \frac{R_{Sample} - R_{Standard}}{R_{Standard}} \times 1000$$

where R stands for the isotopic ratio of the sample and standard, respectively (Craig, 1961a).

Thus, for example if a water has a deuterium delta value, δ^2H of -50 ‰, this means that its deuterium ratio is 50‰ lower than that of the standard. A positive delta value shows that the sample is more enriched in the respective isotope than the standard. Craig (1963) established the isotopic characteristics (δ^2H and $\delta^{18}O$) of precipitation relating to latitude and altitude as well as to continental effects. Samples from higher latitudes and elevation or those collected further inland were progressively lighter (more negative values of δ). The values of δ^2H and $\delta^{18}O$ in precipitation were approximately related by the meteoric water line (Craig, 1961b):

$$\delta^2H = 8\delta^{18}O + 10$$

The expression above is recognised as the *World meteoric line* abbreviated as WML. It describes the global meteoric water line, and in spite of the complex interactions that occur during the meteoric process, there is a remarkably good correlation worldwide. The applications of water isotopes in

geothermal studies do not only involve tracing the origin of water, but are also useful in characterizing the boiling process and in monitoring the flow of injected fluids.

3.2.2 Cl-SO_4-HCO_3 ternary diagram

Relative contents of constituents partitioning into the liquid phase are used in geochemical techniques for specific types of fluids with limited ranges of composition. For example, most ionic solute geothermometers "work" only if used with close to neutral waters containing chloride as the major ion. Any such interpretation of geothermal water samples, therefore, is best carried out on the basis of an initial classification, for example in terms of their major anions Cl^-, SO_4^{-2} and HCO_3^-. Chloride, which is a conservative ion in geothermal fluids, does not take part in reactions with rocks after it has dissolved. That is to say, chloride does not precipitate after it has dissolved; it does not return to the rock so its concentration is independent of the mineral equilibria that control the concentration of the rock-forming constituents. Thus, chloride is used as a tracer in geothermal investigations. The Cl-SO_4-HCO_3 ternary diagram is one diagram for classifying natural waters (Giggenbach, 1991). Using this diagram, several types of thermal water can be distinguished: mature waters, peripheral waters, steam-heated waters and volcanic waters. The diagram provides an initial indication of mixing relationships.

The position of a data point on such a triangular plot is obtained by first establishing the sum of concentrations, C_i ppm (mg/kg), of all three constituents involved:

$$S = C_{Cl} + C_{SO4} + C_{HCO3}$$

The next step is to evaluate the "% - Cl, "% - SO_4" and "% - HCO_3" according to

$$\text{"\% - Cl"} = 100C_{Cl}/S$$

$$\text{"\% - } SO_4\text{"} = 100C_{SO4}/S$$

and

$$\text{"\% - } HCO_3\text{"} = 100C_{HCO3}/S$$

Then, if, *% Cl* is listed in column A, *% SO_4* in column B, and *% HCO_3* in column C in a Grapher (6) worksheet, then column D is prepared as: D = C + 0.5×A. A ternary diagram is plotted such that column A is used for the X-axis and D for the Y-axis.

3.2.3 Cl-Li-B diagram

Lithium is used as a tracer, because it is the alkali metal least affected by secondary processes for initial deep rock dissolution and as a reference for evaluating the possible origin of two important 'conservative' constituents of geothermal waters, Cl and B. Once added, Li remains largely in solution. The B content of thermal fluids is likely to reflect to some degree the maturity of a geothermal system; because of its volatility it is expelled during the early heating up stages. In such a case, fluids from older hydrothermal systems can be expected to be depleted in B (also As, Sb and Hg) while the converse holds for younger hydrothermal systems. It is, however, striking that both Cl and B are added to the Li containing solutions in proportions close to those in crustal rocks. At higher temperatures Cl occurs as HCl and B as H_3BO_3. Both are volatile and able to be mobilized by high-temperature steam. They are, therefore, quite likely to have been introduced with the magmatic vapour invoked above to lead to the formation of a deep acid brine responsible for rock dissolution. At low temperatures the acidity of HCl increases rapidly, and is soon converted by the rock to the less volatile NaCl. B remains in volatile form to be carried in the vapour phase even at lower temperatures. The Cl/B ratio is often used to indicate a common reservoir source for the waters. Care must be taken in applying such interpretation since waters from the same reservoir may show

differences in this ratio, due to changes in lithology at depth over a field (example, the occurrence of a sedimentary horizon), or by the absorption of B into clays during lateral flow.

The position of a data point in such a triangular plot is simply obtained by first establishing the sum S of the concentrations, C_i (in mg/kg), of all three constituents involved:

$$S = C_{Cl/100} + C_{Li} + C_{B/4}$$

The next step consists of the evaluation of "% -Cl", "% -Li" and "% -B/4" according to

$$\text{“\% - } Cl\text{”} = 100C_{Cl/100}/S = C_{Cl}/S$$

$$\text{“\% - } Li\text{”} = 100C_{Li}/S$$

and

$$\text{“\% - } B/4\text{”} = 100C_{B/4}/S$$

Then, if the *% Cl* is listed in column A, *% B/*4 in column B, and *% Li* in column C in a Grapher (6) worksheet, column D is prepared as: D = C + 0.5×A. A ternary diagram is plotted such that column A is used for the X-axis and D for the Y- axis.

3.2.4 Li-Rb-Cs diagram

An indication of the existence of a common origin, or of the common deep process controlling the composition of surface water discharges, is provided by the use of less reactive "conservative" components. These components, such as the rare alkalis Li, Rb and Cs, if added at depth, are not affected by shallow processes. Relative Li, Rb and Cs contents are plotted in terms of a ternary diagram according to:

$$S = C_{Li} + 4C_{Rb} + 10C_{Cs}$$

$$\text{“\% -}Li\text{”} = 100C_{Li}/S$$

$$\text{“\% -}Rb\text{”} = 400C_{Rb}/S$$

and

$$\text{“\% -}Cs\text{”} = 1000C_{Cs}/S$$

In the application of this triangular plot, advantage is taken of its insensitivity to dilution by sparsely mineralized groundwater or steam loss due to boiling of the rising fluids.

3.2.5 Na-K-Mg diagram

This triangular diagram is used to classify waters into fully equilibrated, partially equilibrated and immature waters. It can be used to predict the equilibrium temperature and also the suitability of geothermal waters for application of ionic geothermometers. It is based on the temperature dependence of the full equilibrium assemblage of potassium and sodium minerals that are expected to form after isochemical recrystallization of average crustal rock under conditions of geothermal interest (Giggenbach, 1988). It is essentially based on the temperature dependence of the two reactions.

$$K\text{-feldspar} + Na^+ = Na\text{-feldspar} + K^+$$

$$2.8\ K\text{-feldspar} + 1.6\ water + Mg^{2+} = 0.8\ K\text{-mica} + 0.2\ chlorite + 5.4\ silica + 2\ K^+$$

The position of a data point in this triangular plot is first obtained by establishing the sum of the concentrations C_i (in mg/kg) of all three constituents involved:

$$S = C_{Na}/1000 + C_K/100 + \sqrt{C_{Mg}}$$

$$\text{“\% - Na”} = C_{Na}/10S$$

$$\text{“\% - K”} = C_K/S$$

$$\text{“\% - Mg”} = 100\sqrt{C_{Mg}}/S$$

Then, if, *% Na*/1000 is listed in column A, *% K*/100 in column B and *%* $\sqrt{C_{Mg}}$ in column C in a Grapher (6) worksheet, then column D is prepared as: D = C + 0.5*A. A ternary diagram is plotted such that column A is used as the Y-axis and D as the X- axis.

The area of partial equilibrium suggests either a mineral that has dissolved but not attained equilibrium, or a water mixture that has reached equilibrium (e.g geothermal water) mixed with dilute unequilibrated water (e.g. cold groundwater). Points close to the √Mg corner usually suggest a high proportion of relatively cold groundwater, not necessarily “immature”.

3.3 Geothermometers

The chemical and isotope geothermometers constitute the most important geochemical tool for exploration and development of geothermal resources. During the exploration phase, geothermometers are used to estimate subsurface (below the zone of cooling) temperatures expected to be encountered by drilling, using the chemical and isotopic composition of hot spring and fumarole discharges. When applying these geothermometers, it is invariably assumed that no changes in water composition occur in conjunction with conductive cooling; boiling is taken to be adiabatic (D’Amore and Arnórsson, 2000). When geothermometers are applied to estimate the subsurface temperatures, it is also assumed that temperature-dependent mineral-solution equilibria prevail in the geothermal reservoir.

Geothermometers have been classified into three main groups, namely: water or solute geothermometers, steam or gas geothermometers and isotope geothermometers. Water and steam geothermometers are together termed chemical geothermometers. Different geothermometers are valid for different temperature ranges. The processes that may interfere with and affect different geothermometers differently are: lack of equilibration with a particular mineral, different rates of equilibration between minerals and water, mixing with cold groundwater, boiling and condensation during upflow.

Some temperature equations for silica and cation geothermometers are presented in Appendix I but the most important ones are discussed here below.

3.3.1 Silica (quartz) geothermometers

Silica geothermometers are based on temperature-dependent variations in the solubility of silica species. The solubility of quartz is dependent on pressure, temperature and salinity. The quartz geothermometer works best for waters in the subsurface temperature range 120-250°C (Arnórsson, 2000b). The solubility reactions for silica minerals are invariably expressed as:

$$SiO_2(s) + 2\,H_2O = H_4SiO_4(aq)$$

When using quartz geothermometers, some factors should be considered (Fournier and Potter, 1982):

(i) The temperature range in which the equations are valid;
(ii) Possible polymerization or precipitation of silica before sample collection;

(iii) Possible polymerization of silica after sample collection;
(iv) Control of aqueous silica by solids other than quartz;
(v) The effect of pH upon quartz solubility; and
(vi) Possible dilution of hot water with cold water before the thermal waters reach the surface.

Fournier and Truesdell, (1973) presented a quartz geothermometer with maximum steam loss at 100°C as a function of silica concentration (SiO_2 in mg/kg):

$$t(°C) = \frac{1522}{5.75 - \log\ (SiO_2)} - 273.15$$

The most commonly used formula for the quartz geothermometer (Fournier and Potter, 1982) is:

$$t(°C) = -42.198 + 2.883 \times 10^{-1} S - 3.668 \times 10^{-4} S^2 + 3.1665 \times 10^{-7} S^3 + 70.34 \log S$$

where S = SiO_2 concentration.

The quartz geothermometer may be applicable down to 100°C in old systems, but in young systems, it may not be applicable below 180°C. The expanded formula by Fournier and Potter (1982) is applicable up to 330°C.

3.3.2 Chalcedony geothermometers

The chalcedony geothermometer is based on the solubility of chalcedony (Arnórsson, 1975; Fournier, 1991; Gíslason et al., 1997). Fournier (1991) suggested ambiguity in the use of silica geothermometers below 180°C, as chalcedony appears to control dissolved silica in some areas and quartz in others. Chalcedony is a fine-grained variety of quartz, which is probably not a separate mineral but a mixture of fine-grained quartz and moganite which, with time, probably all changes to quartz (Gíslason et al., 1997). Temperature, time and fluid composition all affect different crystalline forms of silica. Therefore, in some places (old systems) where water has been in contact with rock at a given temperature for a relatively long time, quartz may control dissolved silica at temperatures down to 100°C and chalcedony up to 180°C. The chalcedony geothermometer, at the condition of maximum steam loss presented by Arnórsson et al. (1983), is:

$$t(°C) = \frac{1264}{5.31 - log(SiO_2)} - 273.15$$

and without steam loss

$$t(°C) = \frac{1112}{4.91 - log(SiO_2)} - 273.15$$

3.3.3 Cation geothermometers

Cation geothermometers are based on the temperature dependence of ion exchange or partitioning of alkalis between solutions and solid phases. The reaction involved is appropriately expressed as:

$$NaAlSi_3O_8 + K^+ = KAlSi_3O_8 + Na^+$$

The equilibrium constant for the reaction is:

$$K = \frac{(KAlSi_3O_8)(Na^+)}{(NaAlSi_3O_8)(K^+)}$$

Regarding the respective feldspars as pure, (their activity is approximately 1) and no or equal complexing of Na^+ and K^+ in aqueous solution, and the activity coefficients to be the same for both ions, the equation reduces to:

$$K = \frac{[Na^+]}{[K^+]}$$

where $[Na^+]$ and $[K^+]$ are molalities of respective ions.

The Na-K geothermometer suggested by Giggenbach (1988) is given as:

$$t(°C) = \frac{1390}{1.75 + log\frac{Na}{K}} - 273.15$$

Several authors have suggested empirical Na/K geothermometers based on experiments and obtained different results due to work with different minerals. Basaltic minerals usually give low values (Arnórsson, 1983) but andesitic ones high values (Giggenbach, 1988) at low temperatures. At high temperatures they converge and give similar values. The Na/K ratio works generally well for estimating temperatures of water above 200°C.

The Na-K-Ca geothermometer was developed specifically for calcium-rich waters that give anomalously high calculated temperatures when using the Na-K method. Fournier and Truesdell (1973) developed the equation for the Na-K-Ca geothermometer that has been applied to both low-temperature and high-temperature geothermal reservoirs, expressed as:

$$t(°C) = \frac{1647}{log\frac{Na}{K} + ß\left(log\frac{\sqrt{Ca}}{Na} + 2.06\right) + 2.47} - 2.73.15$$

where β = 4/3, where calculated temperature is > 100°C;
β = 1/3, where calculated temperature is < 100°C.

The Na-K-Ca geothermometer may give erroneous calculated temperatures, as a result of boiling and mixing with cold water. The result of boiling is loss of CO_2 which can cause $CaCO_3$ to precipitate. The Na-K-Ca geothermometer gives anomalously high results when applied to waters rich in Mg^{2+}. Application of an Mg^{2+} correction will lead to an anomalously low calculated reservoir temperature. Thus, chemical geothermometer results should be used with great caution when applied to Mg^{2+}-rich waters (Fournier and Potter, 1979). This problem may also be avoided by the application of the Na-K-Mg diagram (Giggenbach, 1988).

3.4 Solution – mineral equilibrium

The use of multiple mineral equilibria is another method for estimating subsurface temperature in geothermal systems. Reed and Spycher (1984) have suggested that the best estimate of reservoir temperature using geothermometers can be attained by simultaneously considering the state of equilibrium between a specific water and many hydrothermal minerals as a function of temperature. In that case, if a group of minerals converges to equilibrium at a particular temperature, this temperature corresponds to the most likely reservoir temperature. The rising fluid has reacted chemically with rock. The choice of the minerals should include those known to occur as hydrothermal minerals in the area under study or in geothermal systems in general, but particularly those occurring in the same type of rock as the system under exploration. Minerals that should always

be considered include quartz or chalcedony, the alkali feldspars (albite and microcline), calcite, in some cases anhydrite, fluorite and/or zeolites, smectite, chlorite, wairakite, prehnite, epidote and mica. For high-temperature geothermal systems pyrite, pyrrhotite and magnetite should also be considered. The equilibrium state of a mineral can be estimated by the ratio of the reaction quotient (Q) to the equilibrium constant (K). The equilibrium constant and the reaction quotient are related to the Gibbs energy through:

$$\Delta Gr = - RT \ln K + RT \ln Q = RT \ln \left(\frac{Q}{K}\right)$$

where R = Gas constant;
T = Temperature (K)

The saturation index, *SI,* can be obtained from the solubility product and its reaction quotient

$$SI = \log Q - \log K = \log \left(\frac{Q}{K}\right)$$

One of the advantages of this method is that it serves to distinguish between equilibrated and non-equilibrated waters. A large range of temperatures is observed for non-equilibrated waters, as conformity with respect to mineral saturation temperature is generally good for equilibrated waters. All minerals in equilibrium at the same temperature converge to $SI = 0$; $SI < 0$ for an undersaturated solution; $SI > 0$ for supersaturated solutions. If fluid mixes with dilute water, mineral curves will intersect at $SI < 0$, but if it has boiled at $SI > 0$.

Aqueous speciation is calculated at several predetermined temperatures to obtain a log (Q_i/K_i) versus temperature relationship for each mineral for the water composition under consideration. Tole et al. (1993) defined three types of arbitrarily obtained temperatures using the log (Q/K) diagrams: the range of equilibrium temperature is defined as the temperature interval over which at least two minerals attain equilibrium within 4°C of each other; the cluster equilibrium temperature is the range over which most minerals appear to reach equilibrium; and the best equilibrium temperature is the temperature at which the greatest number of minerals is in equilibrium with the aqueous solutions.

Software programs like WATCH (Arnórsson and Bjarnason, 1993) and SOLVEQ (Spycher and Reed, 1989) are generally used to calculate aqueous speciation of geothermal fluids using chemical analyses of samples collected at the surface as input. These programs are used to calculate the equilibrium constant, the reaction quotient and the saturation index for a given reaction at any given temperature. Other parameters include pH, redox potentials, and partial pressures of gases. The state of saturation of many minerals as a function of temperature can be shown by log (Q/K) diagrams.

3.5 Mixing processes

Ascending geothermal waters may cool in upflow zones either by conduction or by boiling due to depressurization, or by both of these processes. However, hot water from a geothermal reservoir may also cool by mixing with shallow cold water. When this happens geothermometers may yield misleading results. Mixing of geothermal water with cold water may take place after a variable amount of conductive cooling of the hot water and before, during or after boiling. Mixing processes such as conductive cooling and boiling can upset the chemical equilibrium between water and rock minerals, thus causing a tendency for the water to change its composition after mixing with respect to reactive chemical components. Chemical analysis of spring waters provides information about which of these processes are taking place in hot spring systems. The dissolved solid concentrations of cold water are most often lower than that of geothermal waters and mixing is often referred to as dilution. Large temperature variations and flowrates of thermal springs in a particular field that can be linked with parallel variations in the concentrations of non-reactive components in the water, such as Cl, usually constitute the best evidence that mixing has occurred.

There are several methods that can be used to infer the mixing of two waters: variation in ratios of conservative elements such as Cl/B, Schoeller diagrams and mixing models. The relationship between chloride and boron appears to be useful for evaluating mixing processes. The linear relationship between these parameters indicates whether mixing has taken place. A linear or near-linear relationship between chloride and silica and sulphate may also be useful to strengthen evidence of mixing. A Schoeller diagram comprises the log concentrations of fluid components from a number of analyses and shows the effects of mixing. Mixing a geothermal with dilute water vertically moves the line representing an analysis without changing its shape (Truesdell, 1991).

Mixing models. Mixing models have been developed to allow for the estimation of a hot water component in mixed waters in springs or discharge from shallow drillholes. Three kinds of mixing models are considered here:

(1) The chloride-enthalpy mixing model, (Fournier, 1977);
(2) The silica-enthalpy mixing model, (Fournier, 1977);
(3) The silica-carbonate mixing model (Arnórsson, 1985).

When applying mixing models to estimate subsurface temperatures, several simplifying assumptions are made. Conservation of mass and heat is always assumed, both during and after mixing. Therefore, it is assumed that chemical reactions occurring after mixing are insignificant and do not modify the water composition.

The chloride-enthalpy model has been widely used. The chloride-enthalpy diagram accounts for both mixing and boiling processes. It works best when initial temperature of the hot water is above 200°C.

The silica-enthalpy mixing model. This diagram may be used to determine the temperature of a hot water component. Truesdell and Fournier (1977) proposed a plot of dissolved silica versus the enthalpy of water to estimate the temperature of the deep hot water component. There are some criteria for hot spring waters which may be appropriate for the application of this model:

(i) A measured water temperature which is at least 50°C less than calculated silica and Na-K-Ca geothermometer temperatures;
(ii) A silica geothermometer temperature which is lower than the Na-K-Ca temperature; and
(iii) A mass flowrate which is high enough to allow for only a little conductive cooling.

This model cannot be used for boiling springs because heat is carried away in the steam after mixing.

The silica-bicarbonate model. This model is based on the relationship between silica and total carbonate concentrations. It is based on the assumption that practically all silica in geothermal water occurs as H_4SiO_4 and all carbonate as CO_2. This model can be used to estimate the temperature of the hot water component in mixed waters and also to distinguish between boiled and non-boiled waters.

4. INTERPRETATION OF DATA ON GEOTHERMAL FLUIDS FROM THE RUNGWE VOLCANIC AREA AND MBEYA REGION IN SW-TANZANIA

The geothermal reservoirs in the Rungwe area are manifested by the presence of thermal springs. Geothermal exploration, however, may reveal hidden reservoirs and serves to locate geothermal areas favourable for development and in finding sites within them for drilling. The principal objective of geochemical surveys during geothermal exploration is to predict subsurface temperatures, to obtain information on the origin of the geothermal fluid and to understand subsurface flow directions (Arnórsson, 2000a). The geothermal-geochemical study of the hot springs in the Mbeya region essentially involves three steps, namely: sampling, analysis and data interpretation.

4.1 Sampling

The field work involved sampling rocks, water and gases. Rock samples included volcanic rocks, xenoliths and travertine deposits. Water samples were collected from cold and hot springs, and from the Ngozi caldera lake. Using glass flasks, gases sampled include carbon dioxide and other reactive gases from bubbling hot and cold springs. Samples intended for analysis of noble gases were collected into special copper tubes. The tubes were placed in the water to prevent atmospheric contamination.

FIGURE 4: Sampling of hot spring water using syringe with filter membrane

For this report thirteen water samples from cold and hot springs and of lake water (Table 1) were used. These samples were collected in June and November, 2006. During sampling, field measurements for pH, conductivity, spring temperature and air temperature were carried out (Table 1). Fu samples (filtered and untreated) were collected for anion determinations. Fa samples (filtered and acidified) acidified with one millilitre of ultra pure concentrated nitric acid, were collected for cation determination. Samples were filtered in the field (Figure 4) through a 0.45 µm filter membrane, and stored in polyethylene bottles. The samples were transported to the Geological Survey of Germany, BGR, for laboratory analysis.

TABLE 1: Water samples from the June and November 2006 field surveys; full analytical results are presented in Appendix II

Location / Sample ID	X-coordinate °East	Y-coordinate °South	Elevation (m)	Date of sampling	Water temp. (°C)	pH lab.	Field conducti. (µS/cm)
Mampulo B	33 47.732	9 32.971	531	8.6.2006	61.0	8.4	7000
Kilambo	33 49.068	9 21.840	632	6.6.2006	56.5	8.3	6000
Ilatile 1	33 12.583	8 53.083	1127	7.6.2006	72.0	8.3	3700
River spring	33 12.565	8 53.010	1087	7.6.2006	74.1	8.3	3700
Ilatile 4	33 12.532	8 53.017	1087	7.6.2006	80.2	8.5	3800
Main spring B	33 10.926	8 52.393	1140	3.11.2006	74.0	7.9	3830
Shiwaga up	33 30.004	9 03.184	1713	4.11.2006	26.5	7.1	140
Mulagara	33 37.743	9 11.705	1470	4.11.2006	26.5	7.1	960
Kandete	33 47.736	9 32.970	537	6.11.2006	56.6	8.1	5450
Kasimulo	33 45.749	9 34.990	512	6.11.2006	54.7	8.0	4330
Isebe	33 39.280	9 12.806	1508	7.11.2006	24.7	7.2	520
Swaya	33 27.748	8 59.342	ca.1810	10.11.2006	44	7.5.	360
Lake Ngozi	33 33.687	9 00.911	ca.2190	11.11.2006	20.9	7.4	4820

4.2 Laboratory analysis

The chemical analysis reported in Appendix II was carried out in the hydrogeochemistry laboratory of Bundesanstalt für Geowissenschaften und Rohstoffe (BGR), Hannover-Germany. The main

components Na, K, Ca, Mg, B, Li, Sr, Al, Si, Mn and Fe were analysed from Fa-sub-samples by Inductively Coupled Plasma Optical Emission Spectroscopy - ICP-OES - based on German standard DIN EN ISO 11885 (1998). Trace components were analysed with Inductively Coupled Plasma Mass Spectrometry - ICP-MS - in three groups:

(i) With low mass resolution (m/Δm=350). This includes Ag, Ba, Be, Cd, Cs, Hf, Hg, In, Mo, Pb, Sb, Sn, Ta, Te, Th, Tl, U, W, Y, and REE;
(ii) With medium resolution (m/Δm=3800) including Al, Bi, Co, Cr, Cu, Ga, Li, Nb, Ni, Rb, Sc, Sr, Ti, V, Zn, and Zr were analysed; and
(iii) With high mass resolution (m/Δm=7500), including As and Se.

Rh was used as an internal standard for all three groups.

The Fu sub-samples were used for anion determination. For the determination of the anions, F^-, Cl^-, Br^-, NO_3^-, SO_4^{2-} an Ion Chromatograph-IC, based on German standard DIN EN ISO 10304-1 (1995) was used. The anion-peaks are detected by electrical conductivity, following neutralization of the alkaline KOH eluent with a membrane suppressor technique. H_2SO_4 was used for regenerating the system. For the determination of alkalinity (acid neutralizing capacity) of a water sample, a 10 ml aliquot of a Fu subsample was titrated with 0.02 N HCl to pH=4.3 (DIN 38409, 1979). The end point was determined potentiometrically using a 2-cell pH-glass electrode. Rocks and gas samples were also analysed at the BGR laboratory but the results are not included in this report. The analytical results for waters from hot springs are presented in Appendix II.

4.3 Classification of samples

Cl-SO_4-HCO_3 ternary diagram: The chemical composition of the waters was investigated using the Cl-SO_4-HCO_3 triangular diagram that is used to classify geothermal water on the basis of major anion concentrations. The data points for hot springs in Figure 5 show two major groups of waters. The first is Lake Ngozi water, which plots close to the mature waters area and is classified as Cl-rich geothermal water. The second group consists of points located in the HCO_3 corner and can be classified as peripheral waters that may have mixed with cold groundwater or CO_2 from a magmatic source. The latter is divided into two distinct groups: thermal waters from Isebe, Shiwaga and Mulagara, which are in the extreme end of the HCO_3 corner; and the thermal waters from Kilambo, Mampulo B, Ilatile 1, River spring, Ilatile 4, Kandete, Main spring, Kasimulo and Swaya which plot near the HCO_3 corner.

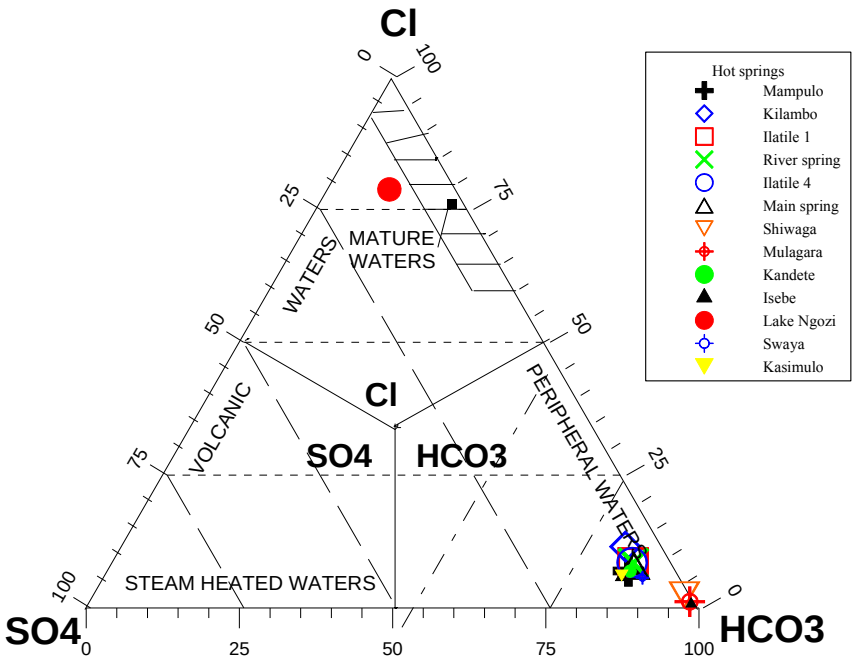

FIGURE 5: Classification of the thermal fluids using Cl-SO_4-HCO_3 diagram

Cl-Li-B diagram: A plot of the relative concentrations of chloride, lithium and boron is shown in Figure 6. Water from Lake Ngozi plots towards the Cl-corner, where mature geothermal water plots. All other hot spring waters plot near the Li-Cl tie line, showing high Cl content relative to Li and B, the area of low absorption of B/Cl steam. This may indicate that they are from old hydrothermal systems and that the fluid migrates from the old basement rock. Water in young systems may plot near the B corner due to the high absorption of B/Cl steam from degassing fresh magma.

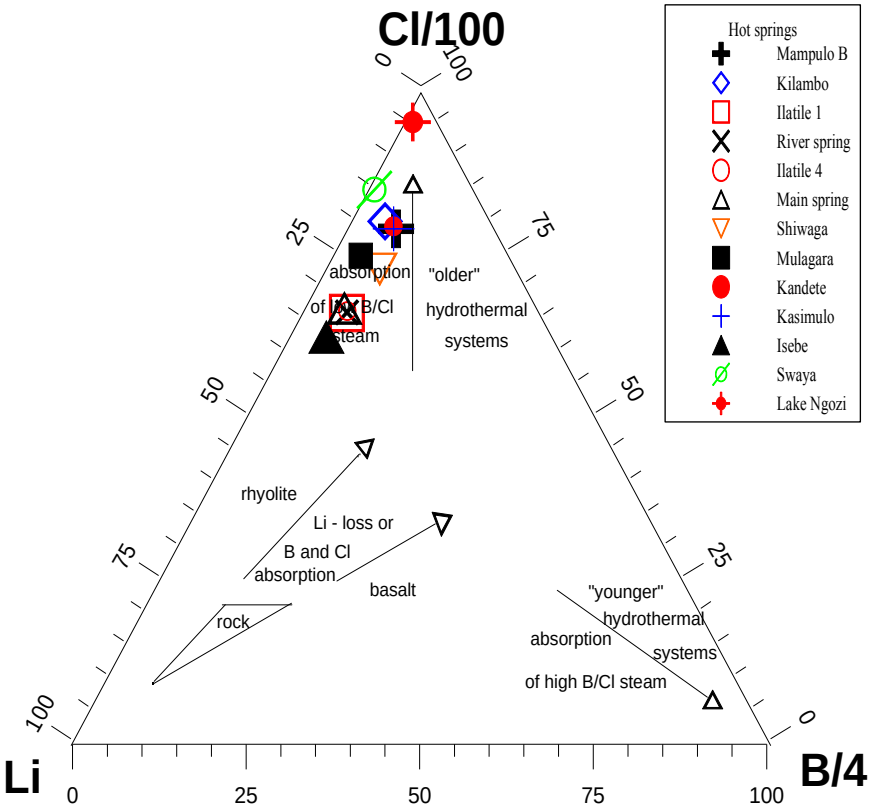

FIGURE 6: Classification of thermal waters using a Cl-Li-B diagram

Na-K-Mg triangular diagram: The diagram using the Na-K equation (Arnórsson et al., 1983) and the K/Mg equation (Giggenbach, 1988) was used for interpretation of analytical data from hot springs. As illustrated in Figure 7, Main spring, Shiwaga, Mulagara, Isebe and Swaya plot in the area of immature waters close to the √Mg corner (with the exception of Main spring, which is not close to the corner). This could mean they have a high proportion of cold groundwater and have not attained equilibrium. For such waters, the application of solute geothermometers to estimate discharge temperature is not suitable. Ilatile 1,

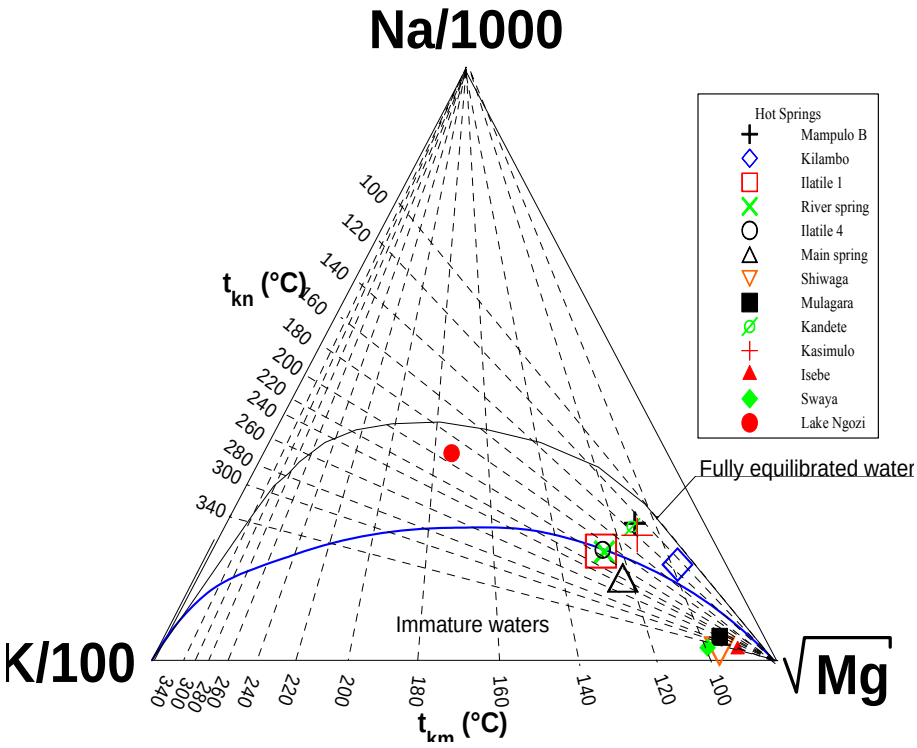

FIGURE 7: The Na-K-Mg tringular diagram for hot springs from Rungwe volcanic area (equation by Arnórsson, 2000a)

River spring and Ilatile 4 plot on the boundary between partially equilibrated and immature waters. This implies that geoindicators can be used on these waters within limits. Kilambo, Kasimulo, Mampulo B, Kandete and Lake Ngozi waters plot in the partial equilibrium area.

4.4 Geothermometry

Chemical geothermometry was used to estimate subsurface temperatures and predict possible cooling in the reservoir during production, as described in Section 3.3. Several of the geothermometer equations are presented in Appendix I. The silica, Na-K, and Na-K-Ca geothermometers were used to estimate subsurface temperature for hot springs and lake water from the Rungwe volcanic area. The WATCH computer program (Bjarnason, 1994) was used for calculations of silica (quartz and chalcedony) and Na-K temperatures. The Na-K-Ca temperature was calculated using the SOLVEQ program (Spycher and Reed, 1989). The measured temperatures of the hot springs and results for solute geothermometry (calculated subsurface temperatures) are summarised in Table 2.

TABLE 2: The results of solute geothermometers, calculations using the WATCH* and SOLVEQ** computer programs; values marked with ? are thought to be unrealistic

Spring	Ionic balance* (%)	Measured $T_{Surface}$ (°C)	T_{quartz}* (°C)	$T_{Chalcedony}$* (°C)	T_{Na-K}** (°C)	$T_{Na-K-Ca}$** (°C)
Mampulo B	3.19	61.0	144	118	131	184
Kilambo	1.91	56.5	147	121	129	175
Ilatile 1	0.96	72.0	112	82	205	221
River spring	3.85	74.1	112	83	203	217
Ilatile 4	0.93	80.2	110	81	201	214
Main spring B	4.14	74	119	90	227	228
Shiwaga	10.55	26.5	122	93	>350?	264?
Mulagara	14.33	26.5	144	118	262?	214?
Kandete	1.93	56.6	147	121	138	186
Kasimulo	-0.97	54.7	137	110	143	182
Isebe	15.14	24.7	145	119	315?	237?
Swaya	7.92	44	131	103	>350?	263?
Lake Ngozi	3.75	20.9	118	89	202	236

Mulagara, Isebe, Shiwaga and Swaya Na-K geothermometer temperatures can be regarded as unrealistic as they fall out of range for the respective geothermometers (Truesdell, 1976; Arnórsson et al., 1983). In Figure 7 they plot in an area which is not suitable for Na-K geothermometry. Mampulo B, Kilambo, Kandete and Kasimulo Na-K temperatures correspond well to those obtained using Arnórsson´s equation (Figure 7). The results for solute geothermometers show that temperatures estimated by the Na-K-Ca geothermometer are much higher (Figure 8) than those estimated by silica and Na-K geothermometers; this could possibly be due to calcium carbonate deposition during upflow which prevents aqueous K and Na from interacting with the country rock (Fournier and Truesdell, 1973). High values are also expected in Mg^{2+} rich waters. Nevertheless the Na-K-Ca geothermometer is best used for waters above 200°C, waters that give anomalously high calculated temperatures when applying the Na-K method.

The calculated quartz geothermometer temperatures for the hot springs give the lowest subsurface temperature of 112°C at Ilatile 1 and the highest temperature of 147°C at Kilambo; the chalcedony geothermometer gives the lowest subsurface temperatures of 81°C at Ilatile 4 and the highest temperature of 121°C at Kilambo; the Na-K geothermometer indicates the lowest subsurface temperature of 129°C at Kilambo and the highest temperature of 227°C at Main spring; while the Na-

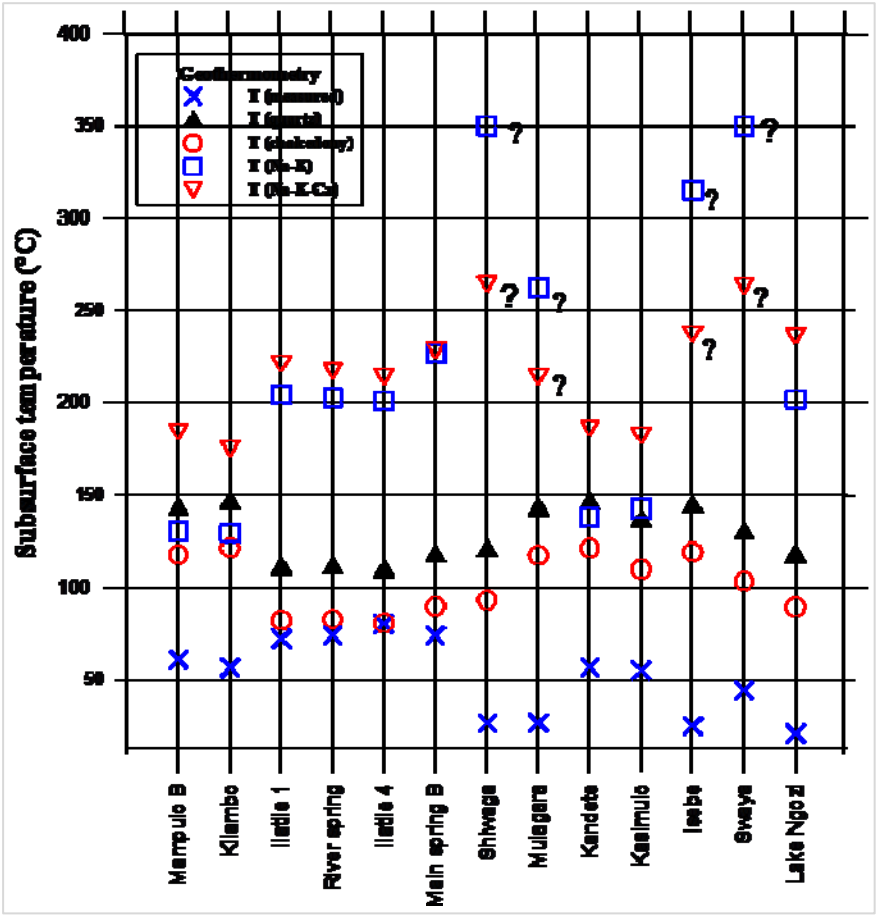

FIGURE 8: Results for geothermometers applied and measured springs temperatures

K-Ca geothermometer suggests 175°C at Kilambo as the lowest subsurface temperature and the highest temperature of 236°C at Lake Ngozi.

4.5 Log (Q/K) diagrams

The SOLVEQ and WATCH computer programs were used to carry out aqueous speciation calculations for samples from each hot spring. Saturation indices with respect to a number of hydrothermal minerals generally present in the geothermal system were calculated as varying temperatures between 25 and 150°C using SOLVEQ. The results were used to plot a saturation index (SI) versus temperature for the minerals selected.

Log (Q/K) vs. temperature diagrams for each hot spring are shown in Figure 9 (13 graphs). The log (Q/K) diagrams for Mulagara, Isebe and Shiwaga show that equilibrium has not been attained, so the subsurface temperature estimations using this method should be interpreted with caution. Their ionic balances as calculated using WATCH are slightly above 10% (Table 2). In Figure 7 they plot in the area of immature waters.

The SI plots (Figure 9) show that no best equilibrium temperatures can be found. This could be due to mixing, degassing, boiling or other processes such as the precipitation of some minerals. For statistical evaluation, the solute-mineral equilibrium temperatures are considered in terms of "range" and "cluster". It should be noted that the range of equilibrium temperatures, the cluster equilibrium temperature and the best temperature were arbitrarily defined as the temperature interval between minimum and maximum equilibrium temperature for selected minerals, the temperature range over which most minerals appear to attain equilibrium, and the temperature at which the greatest number of

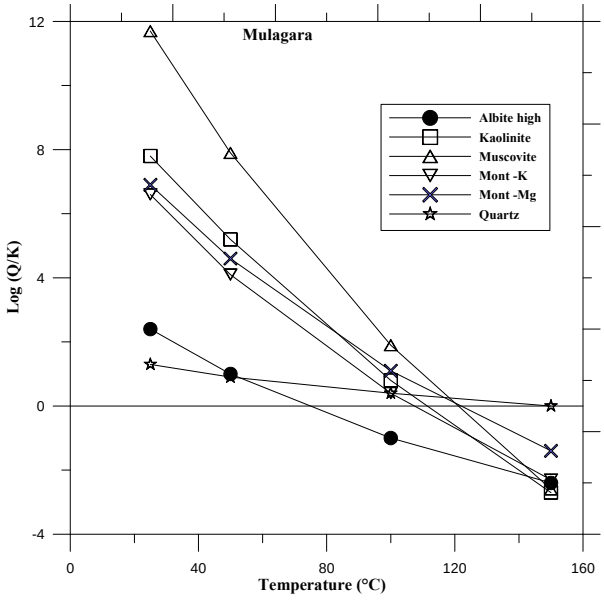

FIGURE 9: Log (Q/K) vs. temperature diagrams for hot springs from the Rungwe volcanic zone, Mbeya, SW-Tanzania

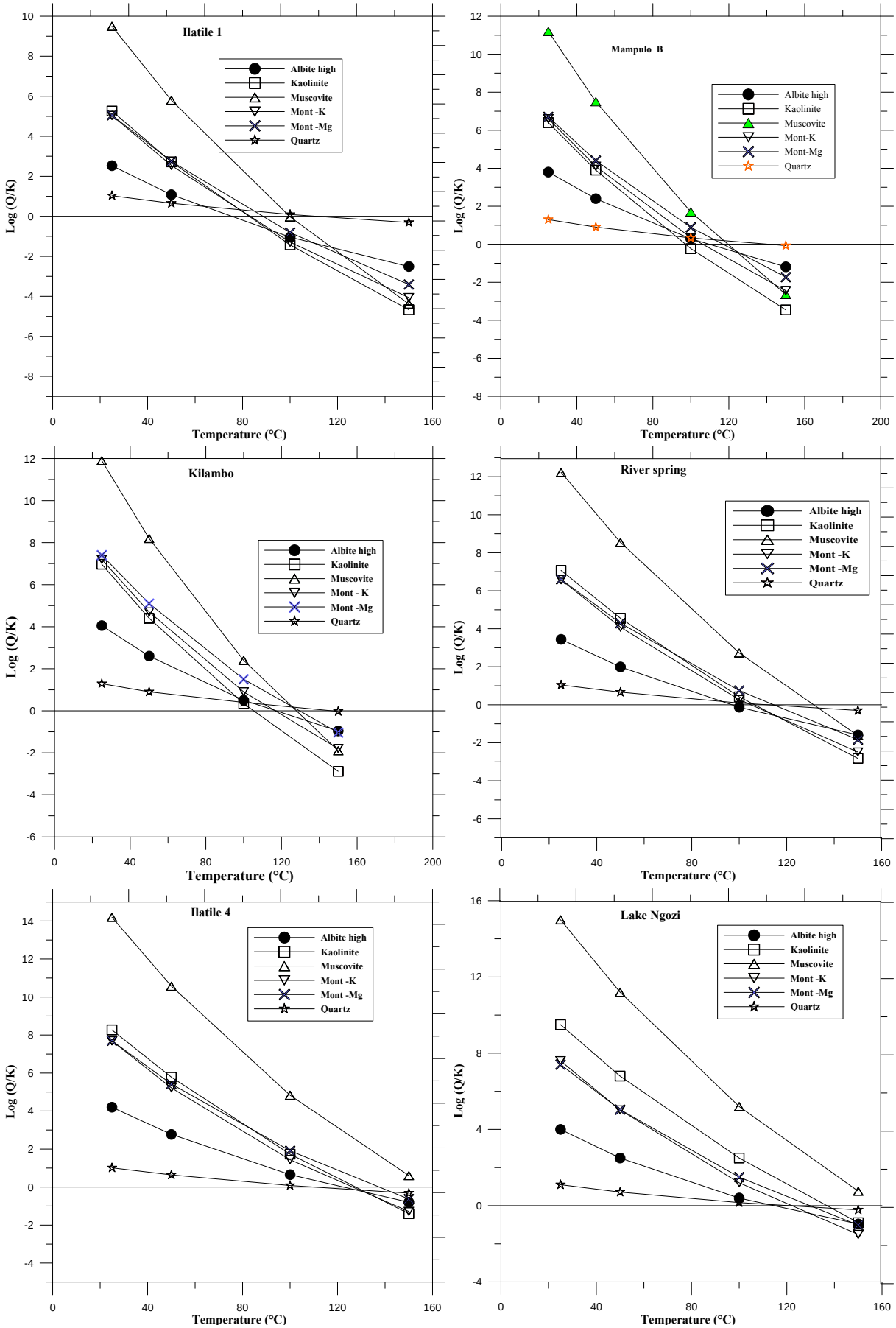

FIGURE 9 cont.: Log (Q/K) vs. temperature diagrams for hot springs from the Rungwe volcanic zone, Mbeya, SW-Tanzania

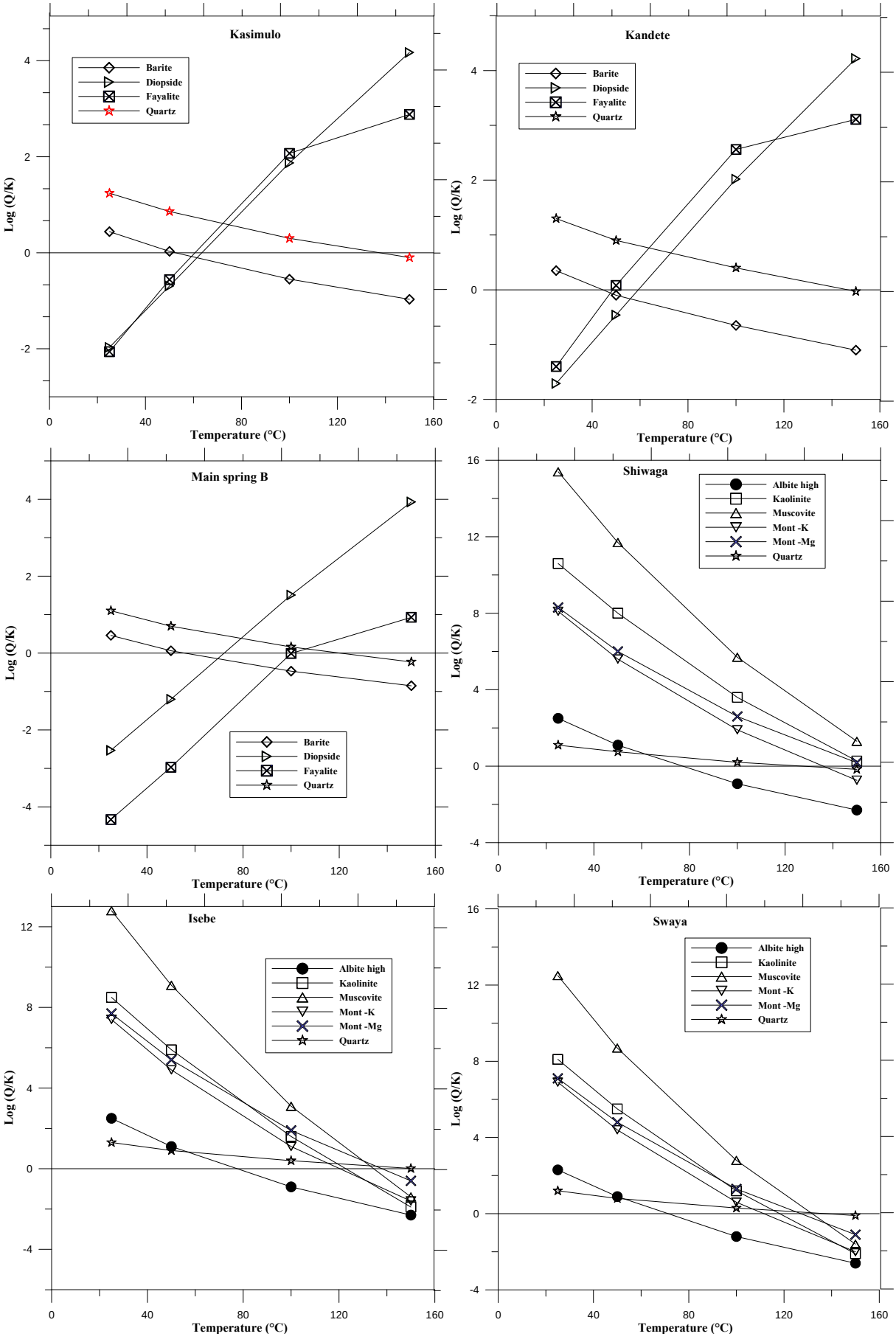

FIGURE 9 cont.: Log (Q/K) vs. temperature diagrams for hot springs from the Rungwe volcanic zone, Mbeya, SW-Tanzania

minerals is in equilibrium with the aqueous solutions, respectively (Tole et al., 1993). With the exception of Kandete and Kasimulo, the chalcedony temperature estimates (Table 2) lie within the subsurface temperature range estimates from the log (Q/K) diagrams (Figure 9).

4.6 Mixing models

Evidence of mixing: Mixing of geothermal water with cold groundwater in shallow zones of hydrothermal systems appears to be common. When mixing occurs, ascending waters may cool by boiling (adiabatically), by conduction or mixing with cold waters in shallow zones. Mixing of geothermal and cold water and the subsequent application of mixing models to estimate subsurface temperatures in geothermal systems depends on the mixing of two components of quite different composition in such a way that the concentrations of reactive components do not change much after mixing has taken place. This kind of mixing is mostly confined to upflow zones. At depth in geothermal reservoirs it is likely that the mixing is completely masked for reactive constituents through re-equilibration of these constituents subsequent to mixing (Arnórsson, 1991). As shown in Figure 5, some of the hot spring waters in the study area may be mixed with cold groundwater. Mixing of two kinds of waters can be shown on a plot of one conservative species against another. A linear relationship between Cl and B in Figure 10 is evidence that the ascending water might have been mixed with cold waters in upflow zones. As Cl is a conservative component in geothermal fluids, its concentration will increase continuously during progressive rock dissolution. A positive linear relationship between Cl and some other selected chemical constituents such as Na, SO_4 and SiO_2 are also observed (Figure 10).

Mixing models: Two mixing models were tested for comparison and further classification of the hot springs in this study, the silica-enthalpy warm spring mixing model (Fournier, 1977) and the silica-carbonate mixing model (Arnórsson, 2000a).

The silica-enthalpy mixing model may be used to determine the temperature of the hot water component, provided silica has not precipitated before or after mixing, and there has been no conductive cooling of the water (Truesdell and Fournier, 1977). Figure 11 depicts the silica-enthalpy mixing model. The cold groundwater sample was assumed to be represented by the available data for chemical composition of river water in the area, from Branchu et al. (2005). A straight line drawn through the data points and extrapolated until it intersects the quartz solubility curve gives the improbably high temperature of 166°C for Kilambo, Kandete and Lake Ngozi; while other points plot between 133 and 166°C (Figure 11). Subsurface temperature estimates using this method are slightly higher than those obtained using the quartz geothermometer (Table 2 and Figure 8) indicating that most of the hot waters have probably mixed with cooler water in the reservoir or that conductive cooling probably took place during the upflow of the hot waters. The mixing model is not applicable in such cases.

The silica-carbonate mixing model is based on the relationship between silica and total carbonate concentrations, assuming that practically all the silica in geothermal systems occurs as H_4SiO_4 and practically all the carbonate carbon as CO_2, and that the concentrations are fixed by temperature dependent solute/mineral equilibrium in the reservoir. This model not only serves to estimate the temperature of the hot water component in mixed waters but also distinguishes boiled and non-boiled waters. When this model is used, points plotted above the curve represent boiled, i.e. degassed waters (degassed of CO_2 but increasing SiO_2), whereas points below the curve correspond to undegassed waters (SiO_2 increases and CO_2 decreases). Figure 12 shows that the points plot below and far from the curve. This means that the hot springs in this study are not boiled. They may be steam-heated waters enriched with emanating CO_2 from the earth. This mixing model cannot be applied in such a case.

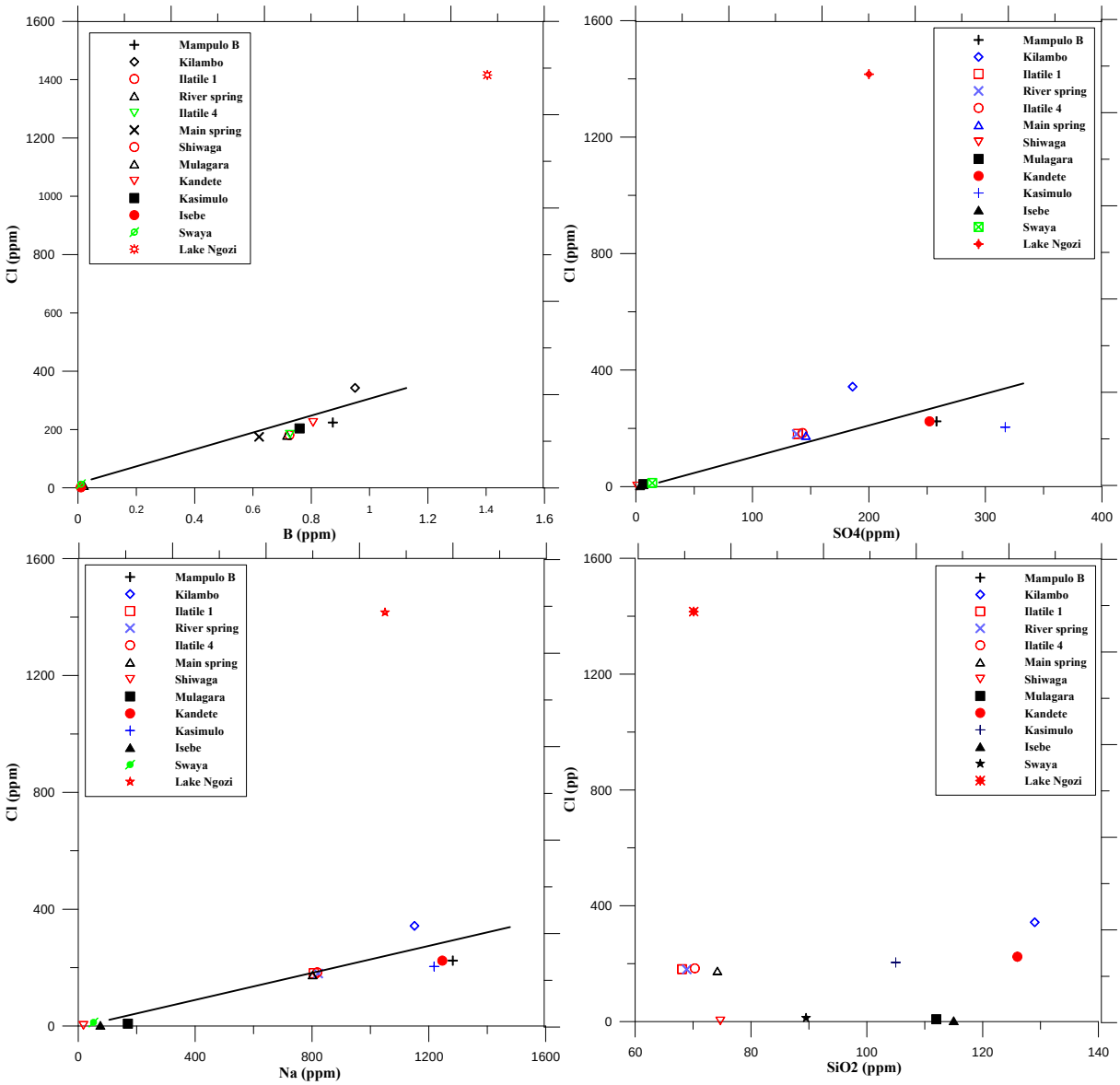

FIGURE 10: Relationships between Cl and B, SO_4, SiO_2 and Na for hot springs from Rungwe volcanic area, Mbeya, SW-Tanzania

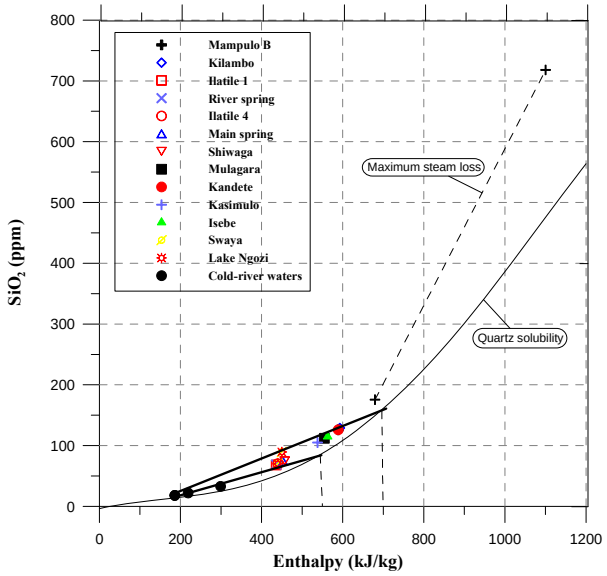

FIGURE 11: The silica-enthalpy plot for the hot springs from the Rungwe volcanic area

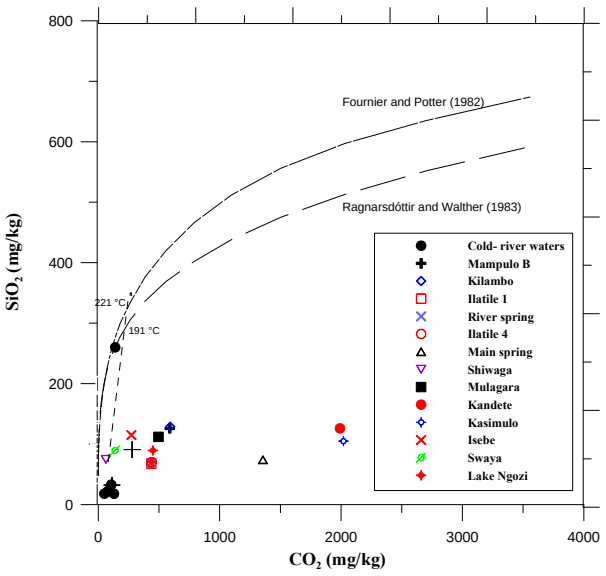

FIGURE 12: The silica-carbonate plot for the hot springs from Rungwe volcanic area

5. CONCLUSIONS

The interpretation of thermal fluids from Tanzania is supported by the presentation of data in triangular diagrams, binary plots, and modelling plots. The advantages of such diagrams is that they allow the immediate "eyeball" statistical evaluation of groupings and trends, but one should bear in mind that any such plot tells only part of the story and that some apparent correlations may be purely fortuitous.

Chemical analyses of water samples from twelve hot springs and one caldera water sample from Lake Ngozi were used for interpretation. No cold groundwater data from the study area were available for studying the fluid flow characteristics to enhance modelling of the geothermal system. Also, stable isotope data for Oxygen-18 (^{18}O) and Deuterium (^{2}H) from the study area were not available. They could have been used for defining the hydrological conditions and evaluating processes that affect the fluids.

Cl-SO_4-HCO_3 and Na-K-Mg ternary diagrams characterise the water from Lake Ngozi as chloride-rich, plotting close to the area of mature geothermal fluids and in the partially equilibrated area. Shiwaga, Mulagara and Isebe are highly carbonated, plotting in the peripheral waters area and immature waters, together with Main spring. With the exception of Main spring, these can be classified as cold springs. Other hot springs are characterised as peripheral waters, plotting in the area of partially equilibrated waters.

The Na-K geothermometer predicts two groups of reservoir temperatures. One categorises Main spring B, Ilatile 1, River spring, Ilatile 4 and Lake Ngozi with subsurface temperatures between 201 and 227°C, and the second group comprises Mampulo B, Kilambo, Kandete and Kasimulo hot springs with subsurface temperatures between 129 and 143°C. Quartz and chalcedony geothermometers predict high subsurface reservoir temperatures of 147 and 121°C, respectively, at Kilambo, and the low subsurface temperatures of 110 and 81°C, respectively, at Ilatile 4.

The silica-enthalpy mixing model, when applied, predicts a subsurface reservoir temperature of 166°C for Kilambo, Kandete and Lake Ngozi. Calculation of mineral saturation indices shows the range and cluster equilibrium temperatures. According to the Cl-Li-B ternary plot, all waters tested have low B/Cl ratios and suggest old hydrothermal systems.

The hot springs studied should be investigated in more detail in order to estimate their potential for energy production and utilization. More investigations are required for establishing potential energy sources for more promising sites. This study, intergrated with studies using TEM, MT and Gravity techniques, isotope ratio and gas methods, can be used to identify exploratory drilling sites.

Study of possible geothermal energy utilization in Mbeya region is highly reccommended.

ACKNOWLEDGEMENTS

I am grateful to the Federal Institute for Geosciences and Natural Resources (BGR), Germany for giving me this opportunity to attend the UNU-GTP specialized training on Chemistry of Geothermal Fluids. I am particularly grateful to the UNU-GTP staff for their tireless assistance, hospitality and kindness, during the application for the fellowships, and the period of my stay in Iceland. Much thanks to my supervisor, Dr. Halldór Ármannsson, all members of staff of ISOR, Orkustofnun and UNU fellows 2007 for their support in numerous ways during the preparation of this report. I am also grateful to my employer, Geological Survey of Tanzania, for granting me the recommendations and permission to participate in the course. I would like to extend my appreciation to Dr. Michael Kraml, BGR, for his encouragement in this course and for making available all the data used in this report.

REFERENCES

Arnórsson, S., 1975: Application of the silica geothermometer in low-temperature hydrothermal areas in Iceland. *Am. J. Sci., 275,* 763-783.

Arnórsson, S., 1983: Chemical equilibria in Icelandic geothermal systems. Implications for chemical geothermometry investigations. *Geothermics, 12,* 119-128.

Arnórsson, S., 1985: The use of mixing models and chemical geothermometers for estimating underground temperature in geothermal systems. *J. Volc. Geotherm. Res., 23,* 299-335.

Arnórsson, S., 1991: Geochemistry and geothermal resources in Iceland, In: D´Amore, F. (co-ordinator), *Applications of geochemistry in geothermal reservoir development.* UNITAR/UNDP publication, Rome, 145-196.

Arnórsson, S. (ed.), 2000a: *Isotopic and chemical techniques in geothermal exploration, development and use. Sampling methods, data handling, interpretation*. International Atomic Energy Agency, Vienna, 351 pp.

Arnórsson, S., 2000b: The quartz and Na/K geothermometers. I. New thermodynamic calibration. *Proceedings of the World Geothermal Congress 2000, Kyushu-Tohoku, Japan,* 929-934.

Arnórsson, S., and Bjarnason, J.Ö., 1993: *Icelandic Water Chemistry Group presents the chemical speciation programme WATCH.* Science Institute, University of Iceland, Orkustofnun, Reykjavík, 7 pp.

Arnórsson, S., Gunnlaugsson, E., and Svavarsson, H., 1983: The chemistry of geothermal waters in Iceland III. Chemical geothermometry in geothermal investigations. *Geochim. Cosmochim. Acta, 47*, 567-577.

Arnórsson, S., Sigurdsson, S., and Svavarsson, H., 1982: The chemistry of geothermal waters in Iceland I. Calculation of aqueous speciation from 0°C to 370°C. *Geochim. Cosmochim. Acta, 46,* 1513-1532.

Bjarnason, J.Ö., 1994: *The speciation program WATCH, version 2.1.* Orkustofnun, Reykjavík, 7 pp.

Branchu, P., Bergonzini, L., Delvaux, D., Batist, M., Golubev, V., Beneditti, M., and Klerk, J., 2005: Tectonic, climatic and hydrothermal control on sedimentation and water chemistry of northern Lake Malawi (Nyasa), Tanzania. *J. African Earth Science, 43,* 433-446.

Craig, H., 1961a: Standards for reporting concentrations of deuterium and oxygen-18 in natural waters. *Science, 133*, 1833-1834.

Craig, H., 1961b: Isotopic variations in meteoric water. *Science, 133*, 1702-1703.

Craig, H., 1963: The isotopic geochemistry of water and carbon in geothermal areas. In: Tongiorgi, E. (ed.), *Nuclear geology on geothermal areas*. Consiglio Nazionale delle Ricerche, Laboratorio di Geologia Nucleare, Pisa, 17-53.

D'Amore, F., and Arnórsson, S., 2000: Geothermometry. In: Arnórsson, S. (ed.), *Isotopic and chemical techniques in geothermal exploration, development and use. Sampling methods, data handling, and interpretation*. International Atomic Energy Agency, Vienna, 152-199.

DECON, SWECO, and Inter-Consult, 2005: *Tanzania rural electrification study – technical report on geothermal power, Activity 1.4.1.* Ministry of Energy and Minerals & Tanzania Electric Supply Company Ltd., report.

Delvaux, D.F and Hanon, M., 1993: Neotectonics of the Mbeya area, SW-Tanzania. *Mus. Roy. Afri. Centr., Tervuren (Belg.), Dept. Geol. Min., Rapp. Ann. 1991-1992*, 87-97.

Ebinger, C.J., Deino, A.L., Drake, R.E., and Tesha, A.L., 1989: Chronology of volcanism and rift basin propagation: Rungwe volcanic province, East Africa. *J. Geophys. Res., 94 B11:15*, 785-803.

Fournier, R.O., 1977: Chemical geothermometers and mixing models for geothermal systems. *Geothermics, 5,* 41-50.

Fournier, R.O., 1991: Water geothermometers applied to geothermal energy. In: D'Amore, F. (coordinator), *Application of geochemistry in geothermal reservoir development*. UNITAR/UNDP publication, Rome, 37-69.

Fournier, R.O., and Potter, R.W. II, 1979: Magnesium correction to the Na-K-Ca geothermometer. *Geochim. Cosmochim. Acta, 43,* 1543-1550.

Fournier, R.O., and Potter, R.W., 1982: An equation correlating the solubility of quartz in water from 25° to 900°C at pressures up to 10,000 bars. *Geochim. Cosmochim Acta, 46*, 1969-1973

Fournier, R.O., and Truesdell, A.H., 1973: An empirical Na-K-Ca geothermometer for natural waters. *Geochim. Cosmochim. Acta*, *37*, 1255-1275.

Giggenbach, W.F., 1988: Geothermal solute equilibria. Derivation of Na-K-Mg-Ca geoindicators. *Geochim. Cosmochim. Acta, 52*, 2749-2765.

Giggenbach, W.F., 1991: Chemical techniques in geothermal exploration. In: D'Amore, F. (coordinator), *Application of geochemistry in geothermal reservoir development*. UNITAR/UNDP publication, Rome, 119-142.

Gíslason, S.R., Heaney, P.J., Oelkers, E.H., and Schott, J., 1997: Kinetic and thermodynamic properties of moganite, a novel silica polymorph. *Geochim. Cosmochim. Acta, 61,* 1193-1204.

Harkin, D.A., 1960: *The Rungwe volcanics at the northern end of Lake Nyasa*. Geological Survey of Tanganyika, MEMOIR II, Dar es Salaam, 172 pp.

Hochstein, M.P., 2005: Heat transfer by hydrothermal systems in the East African Rift. *Proceedings of the World Geothermal Congress 2005, Antalya, Turkey,* CD 7 pp.

Hochstein, M.P., Temu, E.B, and Moshy, C.M.A., 2000: Geothermal resources of Tanzania. *Proceedings of the World Geothermal Congress 2000, Kyushu-Tohoku, Japan*, 1233-1238.

James, T.C., 1967: Thermal springs in Tanzania, discussion and contribution. *Trans. Instn Min. Metak, 76,* B1-18.

Makundi, J.S, and Kifua, G.M., 1985: Geothermal features of the Mbeya prospect in Tanzania. *Geothermal Resources Council, Trans., 9-1,* 451-454.

McNitt, J.R., 1982: The geothermal potential of East Africa. *UNESCO/USAID Geothermal Seminar, Nairobi, Kenya, June 15-21,* 1-9.

Mnzava, L.J., Mayo, A.W., and Katima, J.H.Y., 2004: In search of geothermal energy power potential in Tanzania: the role of geophysics. *Geo-Environment, WIT Press*, 25-36.

Mwihava, N.C.X., Mbise, H.A., and Kibakaya, G., 2004: *Geothermal energy potential in Tanzania.* African Energy Policy Research Network, Nairobi.

Pisarskii, B.I., Konev, A.A., Levi, K.G., and Delvaux, D., 1998: Carbon dioxide-bearing alkaline hydrotherms and strontium-bearing travertines in the Songwe River Valley (Tanzania) (in Russian). *Geologiya i Geofizika 39-7,* 941-948.

Reed, M.H., and Spycher, N.F., 1984: Calculation of pH and mineral equilibria in hydrothermal water with application to geothermometry and studies of boiling and dilution. *Geochim. Cosmochim. Acta, 48*, 1479-1490.

Spycher, N.F., and Reed, M.H., 1989: *User´s guide for SOLVEQ: A computer program for computing aqueous-minerals-gas equilibria (revised prelim. edition).* University of Oregon, Eugene, OR, 37 pp.

SWECO, 1978: *Reconnaissance of geothermal resources*. Report for the Ministry of Water, Energy and Minerals of Tanzania, SWECO, Stockholm, Sweden, 51 pp.

Tole, M.P., Ármannsson, H., Pang Z.H., and Arnórsson, S., 1993: Fluid/mineral equilibrium calculations for geothermal fluids and chemical geothermometry. *Geothermics, 22*, 17-37.

Truesdell, A.H., 1976: Summary of section III - geochemical techniques in exploration. *Proceedings of the 2nd U.N. Symposium on the Development and Use of Geothermal Resources, San Francisco, 1,* liii-lxxix.

Truesdell, A.H., 1991: Effects of physical processes on geothermal fluids. In: D'Amore, F. (coordinator), *Application of geochemistry in geothermal reservoir development.* UNITAR/UNDP publication, Rome, 71-92.

Truesdell, A.H., and Fournier, R.O., 1977: Procedure for estimating the temperature of a hot water component in a mixed water using a plot of dissolved silica vs. enthalpy. *U.S. Geol. Survey J. Res., 5,* 49-52.

Walker, B.G., 1969: Springs of deep seated origin in Tanzania. *Proceedings of the 23rd International Geological Congress, 19,* 171-180.

APPENDIX I: Temperature equations for silica and cation geothermometers

S represents silica concentration as SiO_2 in mg/kg.
Concentrations for cations are in ppm if not specified.

Quartz geothermometers

1. Fournier and Potter (1982); range 20-330°C:

$$t\,(°C) = C_1 + C_2S + C_3S^2 + C_4S^3 + C_5\,logS$$

where $C_1 = -4.2198 \times 10^{1}$, $C_2 = 2.8831 \times 10^{-1}$, $C_3 = -3.6686 \times 10^{-4}$
$C_4 = 3.1665 \times 10^{-7}$, $C_5 = 7.7034 \times 10^{1}$, $S = SiO_2$

2. Fournier (1977), range 25-250°C, no steam loss:

$$t(°C) = \frac{1309}{5.19 - logS} - 273.15$$

3. Fournier (1977), range 25-250°C, after steam loss at 100°C:

$$t(°C) = \frac{1522}{5.75 - logS} - 273.15$$

4. Arnórsson et al. (1983), no steam loss:

$$t(°C) = \frac{1164}{4.90 - logSiO_2} - 273.15$$

Chalcedony geothermometers

5. Fournier (1977), range 0-250°C, no steam loss:

$$t(°C) = \frac{1032}{4.69 - logSiO_2} - 273.15$$

Na/K geothermometers

6. Truesdell (1976), range 100-275°C:

$$t(°C) = \frac{856}{0.857 + \log\ (\mathrm{Na/K})} - 273.15$$

$$t(°C) = \frac{933}{0.993 + \log\ (\mathrm{Na/K})} - 273.15$$

7. Fournier and Potter (1979):

$$t(°C) = \frac{1217}{1.483 + \log\ (\mathrm{Na/K})} - 273.15$$

8. Giggenbach (1988):

$$t(°C) = \frac{1390}{1.750 + \log\ (\mathrm{Na/K})} - 273.15$$

9. Fournier and Truesdell (1973):

$$t(°C) = \frac{777}{0.70 + \log\ (\mathrm{Na/K})} - 273.15$$

Na-K-Ca geothermometer

10. Fournier and Truesdell (1973):

$$t(°C) = \frac{1647}{\log\ (\mathrm{Na/K}) + ß\ \left[\log\left(\sqrt{\mathrm{Ca/Na}}\right) + 2.061\right] + 2.47} - 273.15$$

where ß = 4/3 for t <100°C, and ß = 1/3 for t >100°C

Magnesium correction to the Na-K-Ca geothermometer is given by:

$$\frac{C_{Mg}}{C_{Mg+}\ 0.61 C_{Ca+}\ 0.31\ C_K} \times 100$$

In the equations, C_x and T represent the concentration of component x in ppm and Na-K-Ca temperature in K, respectively.

For 1.5<R<5 the Mg correction, Δt_{Mg} (°C) is:

$$\Delta t_{Mg} = -1.03 + 59.971 \times \log R + 145.05 \times (\log R)^2 - 36711 \text{ x } (\log R)^2/\mathrm{T} - 1.67 \times 10^7 \text{ x } \log R/T^2$$

For 5<R<50

$$\Delta t_{Mg} = 10.66 - 4.7415 \times \log R + 325.87 \times (\log R)^2 - 1.0332 \times 10^5\ (\log R)^2/T - 1.968 \times 10^7 \times \log R/T^2 + 1.605 \times 10^7 \times (\log R)^3/T$$

Do not apply a Mg correction if Δt is negative or R<1.5.

APPENDIX II: Analytical results of water samples from springs and lake water in Mbeya, SW-Tanzania

Sample ID	F	Cl	SO_4	HCO_3	NO_3	CO_3	PO_4	NO_2	NH_4	BO_2	Br	K	Na	Mg	Ca	Al	Co	Cu
	mg/l	mg/l	mg/l	mg/l	mg/l	mg/l	mg/l	mg/l	mg/l	mg/l	mg/l	mg/l	mg/l	mg/l	mg/l	mg/l	µg/l	µg/l
Mampulo B		224	258	2610	<0.01	120	0.58	0.97		3.46	<0.01	62.1	1282	14	12.5	0.02	0.04	0.27
Kilambo		343	186	2410	<0.01	30	0.1	1.32		3.76	<0.01	54.8	1151	30.8	22	0.028	0.18	0.21
Ilatile 1		181	139	1760	0.02	54	0.05	<0.01		2.87	0.79	83.4	806	7.9	10.4	0.007	<0.02	0.15
River spring		180	138	1730	0.38	78	0.02	0.03		2.84	0.79	83.5	821	8.5	15.9	0.056	0.06	0.27
Ilatile 4		184	143	1760	0.04	66	0.03	<0.01		2.88	0.81	82	818	8	17.1	0.371	0.15	1.05
Main Spr.B		175	146	1880	<0.10		<0.03		0.16	2.46	0.7	102	802	16.2	21	<0.005	0.03	0.15
Shiwaga uphill	0.39	2.2	1.05	86.8	0.4		<0.03		0.06	0.04	<0.03	9.7	17.7	1.2	6.5	0.181	0.38	0.06
Mulagara	0.29	8.3	6.42	687	3.7		0.74		0.01	0.08	0.03	29.4	170	15.1	42.9	0.005	0.04	0.2
Kandete		224	252	2760	<0.10		0.58		0.07	3.19	1.02	66	1246	13.9	15.5	<0.005	<0.02	0.42
Kasimulo		204	317	2800	<0.10		0.68		<0.01	3.01	0.94	68.1	1218	15.8	26.1	<0.005	0.48	0.62
Isebe	0.38	2.9	3.47	379	<0.10		0.63		<0.01	0.04	0.01	21.4	75.7	16.3	27.2	0.014	0.02	0.07
Swaya	0.43	12.5	14	193	2.3		0.08		<0.01	0.04	0.06	23.8	52.1	4.8	13.1	0.019	0.03	0.27
Lake Ngozi		1416	200	181	<0.10		0.33		0.01	5.56	4.6	106	1050	0.9	4.2	0.108	0.01	0.15

Sample ID	Fe	Li	Mn	Ni	Pb	Sr	Zn	SiO_2	Ag	As	Ba	Be	Bi	Cd	Ce	Cr	Cs	Dy
	mg/l	mg/l	µg/l	µg/l	µg/l	mg/l	µg/l	mg/l	µg/l	µg/l	mg/l	µg/l	µg/l	µg/l	µg/l	µg/l	µg/l	µg/l
Mampulo B	0.285	0.414	13.9	0.11	<0.100	2.88	<0.4	126	<0.004	131.6	0.092	0.521	<0.002	0.035	0.032	0.09	12.209	0.0025
Kilambo	0.119	0.671	2.5	1.17	<0.100	3.32	0.6	129	<0.004	205.9	0.124	0.667	<0.002	0.027	0.112	0.08	13.085	0.0059
Ilatile 1	0.011	0.758	<1.00	0.19	<0.100	6.84	<0.4	68.1	<0.004	143.3	0.172	10.3	0.003	0.052	0.004	0.03	57.069	<0.0010
River spring	0.03	0.751	1.6	0.28	<0.100	8.07	<0.4	68.9	<0.004	140.8	0.172	10.4	<0.002	0.038	0.212	0.07	54.636	0.0078
Ilatile 4	0.177	0.762	3.8	0.4	0.243	6.89	1	70.3	<0.004	148.5	0.17	9.035	0.004	0.041	1.606	0.38	58.77	0.0428
Main Spr. B	0.024	0.725	<0.50	0.85	<0.050	8.66	0.2	74.2	0.004	112.8	0.149	5.448	0.001	0.028	0.002	0.05	35.91	<0.0005
Shiwaga uphill	0.281	0.006	1358	0.53	0.07	0.15	8.1	74.7	<0.002	<0.3	0.004	0.821	0.003	0.048	1.143	0.08	0.17	0.0448
Mulagara	0.461	0.024	79	0.35	0.09	0.34	2.2	112	<0.002	0.5	0.005	0.486	0.002	0.036	0.027	0.09	0.093	0.005
Kandete	0.254	0.418	11.4	0.21	<0.100	2.56	<0.4	126	0.004	100.7	0.089	0.651	0.007	0.019	0.004	0.06	9.424	<0.0010
Kasimulo	0.206	0.386	35.6	1.2	<0.100	2.37	0.6	105	<0.004	69.6	0.09	0.184	0.034	0.022	0.041	0.06	5.705	0.0073
Isebe	0.077	0.015	54	0.11	<0.050	0.17	2.2	115	0.002	0.5	0.007	1.048	0.007	0.05	0.044	0.12	0.11	0.0054
Swaya	0.027	0.022	10.4	0.24	0.06	0.13	0.6	89.5	<0.002	1	0.027	0.137	0.005	0.009	0.184	2.11	0.504	0.0057
Lake Ngozi	0.007	0.653	10.3	0.2	0.45	0.2	0.5	70.1	0.002	74.2	0.006	2.273	0.038	0.04	0.148	0.17	49.79	0.0045

Sample ID	Er	Eu	Ga	Gd	Ge	Hf	Ho	In	La	Lu	Mo	Nb	Nd	Pr	Rb
	µg/l	µg/l	µg/l	µg/l	µg/l	µg/l	µg/l	µg/l	µg/l	µg/l	µg/l	µg/l	µg/l	µg/l	µg/l
Mampulo B	0.0025	0.0066	0.14	0.0015	14.05	<0.002	<0.0010	<0.004	0.022	<0.0010	15.497	0.018	0.0153	0.0043	162.6
Kilambo	0.0044	0.0117	0.068	0.003	17.89	0.003	0.0013	<0.004	0.059	<0.0010	13.121	0.061	0.0492	0.012	187.6
Ilatile 1	<0.0010	0.0133	0.236	<0.0010	21.86	0.003	<0.0010	<0.004	0.005	<0.0010	19.09	0.009	0.003	<0.0010	368.7
River spring	0.0053	0.0221	0.224	0.0063	23.34	0.018	0.0018	<0.004	0.132	<0.0010	18.147	0.147	0.0749	0.0243	356.6
Ilatile 4	0.0236	0.0267	0.22	0.0493	24.19	0.062	0.0102	<0.004	0.998	0.0052	19.302	0.858	0.5773	0.1807	381.3
Main Spr.B	0.0006	0.0164	0.127	<0.0005	22.34	0.006	<0.0005	<0.002	0.004	<0.0005	13.07	0.008	0.0031	0.0008	382
Shiwaga uphill	0.0442	0.0139	0.02	0.0022	<0.30	0.009	0.0109	<0.002	0.785	0.0142	0.353	0.109	0.9424	0.1593	44.3
Mulagara	0.0063	0.0008	0.008	0.0019	<0.30	0.002	0.0017	<0.002	0.033	0.0034	3.336	0.444	0.027	0.0061	80.7
Kandete	<0.0010	0.01	0.059	0.001	15.6	<0.002	<0.0010	<0.004	0.005	<0.0010	9.804	<0.002	0.0055	<0.0010	157
Kasimulo	0.01	0.0086	0.136	0.0076	9.04	0.003	0.0017	<0.004	0.022	0.0018	8.149	0.014	0.0348	0.0058	142
Isebe	0.0022	0.0009	0.017	0.0009	<0.30	<0.001	0.0014	<0.002	0.047	0.0023	3.198	0.193	0.0354	0.0069	49.9
Swaya	0.0023	0.0021	0.045	<0.0005	0.38	0.003	0.001	<0.002	0.097	0.0008	1.705	0.119	0.0902	0.0156	59.7
Lake Ngozi	0.0024	0.0021	0.051	<0.0005	13.6	0.007	0.0018	<0.002	0.093	0.0009	28.3	0.15	0.107	0.0155	787

Sample ID	Sb	Sc	Sc	Se	Sm	Sn	Ta	Tb	Te	Th	Ti	Tl	Tm	U	V
	µg/l	µg/l	µg/l	µg/l	µg/l	µg/l	µg/l	µg/l	µg/l	µg/l	µg/l	µg/l	µg/l	µg/l	µg/l
Mampulo B	0.079	0.172	0.172	<10	0.0022	<0.04	<0.002	<0.0010	0.03	0.0055	0.66	0.3	<0.0010	0.6102	0.51
Kilambo	0.544	0.071	0.071	<10	0.0082	<0.04	0.002	<0.0010	0.027	0.0105	1.07	0.604	<0.0010	1.3362	0.08
Ilatile 1	1.524	<0.016	<0.016	<10	<0.0020	<0.04	0.004	<0.0010	0.031	0.0015	<0.02	1.447	<0.0010	0.8089	0.06
River spring	1.135	0.058	0.058	<10	0.0099	<0.04	0.011	<0.0010	0.021	0.0318	1.96	1.35	<0.0010	0.8293	0.37
Ilatile 4	1.003	0.171	0.171	<10	0.0887	0.05	0.048	0.0095	0.012	0.2068	17	1.499	0.0039	0.8382	1.09
Main Spr.B	0.399	0.131	0.131	<5	0.0013	0.05	<0.001	<0.0005	0.035	0.035	<0.01	1.492	<0.0005	1.179	0.09
Shiwaga uphill	0.01	0.115	0.115	<5	0.1182	0.04	0.002	0.0017	0.009	0.019	0.77	0.124	0.0134	0.072	0.04
Mulagara	0.006	0.254	0.254	<5	0.0038	0.04	<0.001	<0.0005	0.006	0.006	0.2	0.03	0.0024	5.011	1.7
Kandete	0.051	0.235	0.235	<10	<0.0020	0.07	<0.002	<0.0010	0.037	0.009	<0.02	0.344	<0.0010	0.328	0.14
Kasimulo	0.021	0.16	0.16	<10	0.006	0.09	<0.002	0.0013	0.022	0.067	<0.02	1.14	0.0018	0.98	0.83
Isebe	0.011	0.118	0.118	<5	0.0042	0.06	<0.001	<0.0005	0.007	0.008	0.23	0.022	0.0021	2.48	1.52
Swaya	0.031	0.069	0.069	<5	0.0134	0.1	0.002	<0.0005	0.007	0.013	1.32	0.028	0.001	0.714	4.27
Lake Ngozi	2.182	0.097	0.097	10	0.0142	0.08	0.002	<0.0005	0.022	0.097	0.49	0.608	0.0014	0.121	0.58

Sample ID	W	Y	Yb	Zr	Cond. calc.	Cond. lab	Cond. field	pH field	pH lab	Temperat. water	Temp. air
	µg/l	µg/l	µg/l	µg/l	[µS/cm]	[µS/cm]	[µS/cm]			[°C]	[°C]
Mampulo B	1.462	0.06	0.0018	0.157	4973		7000	n.a.	8.4	61.0	n.a.
Kilambo	0.192	0.074	0.0022	0.107	4630		6000	6.6	8.3	56.5	n.a.
Ilatile 1	6.895	0.092	<0.0010	0.027	3276		3700	10.5	8.3	72.0	n.a.
River spring	5.58	0.146	0.0047	0.745	3344		3700	9.8	8.3	74.1	n.a.
Ilatile 4	6.624	0.357	0.03	3.055	3346		3800	9.5	8.5	80.2	n.a.
Main Spr.B	0.547	0.127	<0.0005	0.033	3316	3550	3830	ca. 7	7.9	74	n.a.
Shiwaga uphill	0.006	0.64	0.0828	0.56	139	141	140	8.46	7.1	26.5	n.a.
Mulagara	0.016	0.126	0.0185	0.615	945	1047	960	6.1	7.1	26.5	23.8
Kandete	1.329	0.05	0.0015	0.098	4768	5070	5450	7.4	8.1	56.6	n.a.
Kasimulo	0.15	0.156	0.0113	0.12	4831	5080	4330	7.7	8	54.7	n.a.
Isebe	0.008	0.113	0.0119	0.166	556	590	520	8.2	7.2	24.7	23
Swaya	0.307	0.052	0.0046	0.166	364	390	360	7.2	7.5	44	26
Lake Ngozi	60.9	0.073	0.0067	0.179	4904	5330	4820	7.15	7.4	n.a.	20.9.